

Simulating Pervasive Fracture Processes In Quasi-brittle Materials Using Random Polyhedral Finite Elements

Joe Bishop
Computational Structural Mechanics
Sandia National Laboratories
Albuquerque, NM 87185

Presented at the 2010 Engineering Mechanics Institute Conference
August 9-11, 2010, Los Angeles

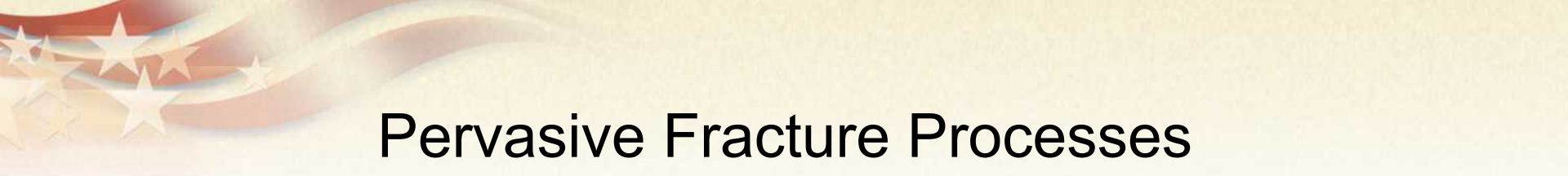
Sandia National Laboratories is a multi-program laboratory operated by Sandia Corporation, a wholly owned subsidiary of Lockheed Martin Corporation, for the U.S. Department of Energy's National Nuclear Security Administration under contract DE-AC04-94AL85000



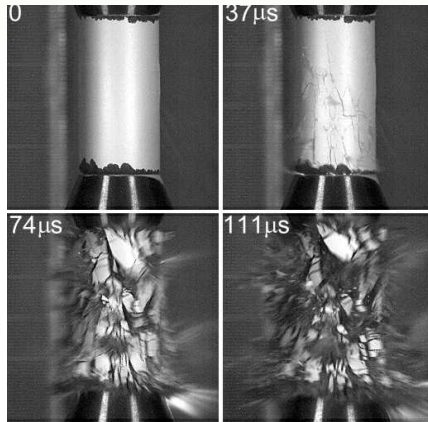


Outline

1. Pervasive fracture modeling approach
2. Randomly close-packed Voronoi tessellations
3. Polyhedral element formulations
4. Statistical mesh convergence
5. Applications
6. Summary



Pervasive Fracture Processes



dynamic pervasive fracture



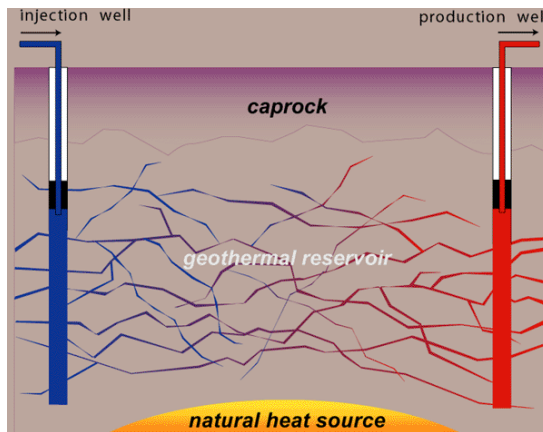
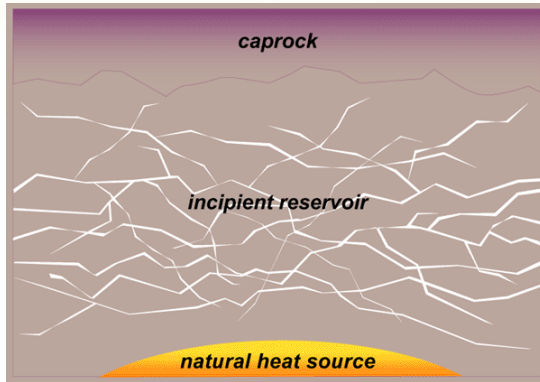
blast induced structural collapse



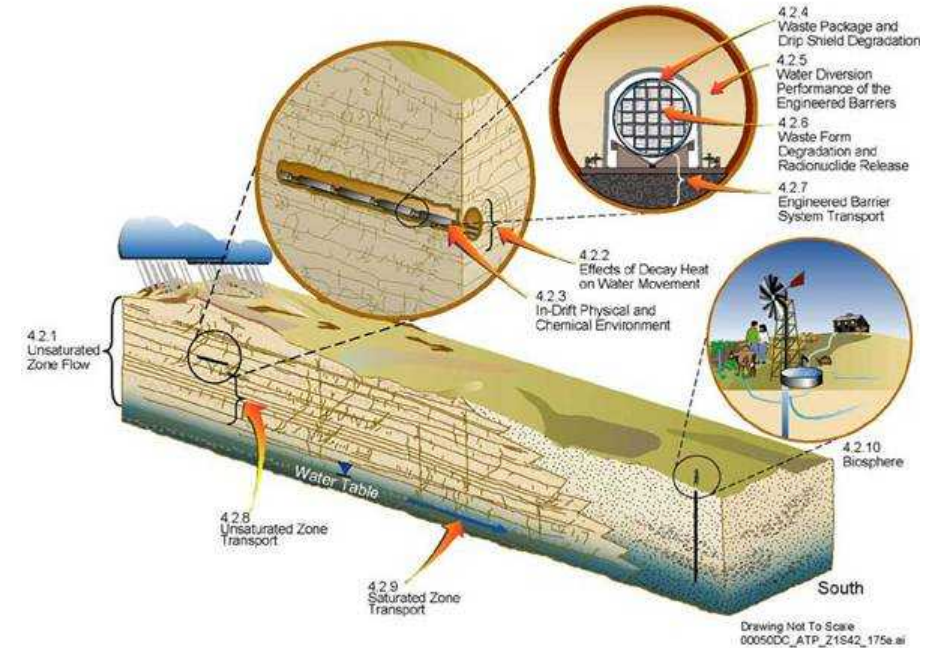
cool picture of dried clay

Fluid Flow on Discrete Fracture Networks

engineered geothermal

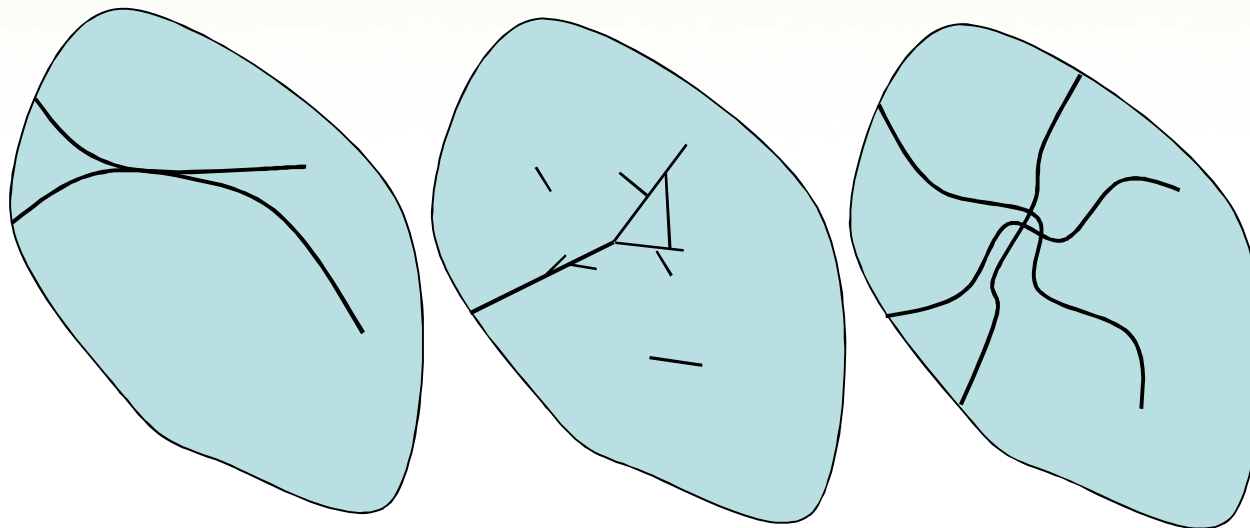


nuclear waste isolation,
CO₂ sequestration





Computational Challenges of Allowing Cracks to Grow Arbitrarily



- Do we restrict branching?
- Do we restrict initiation?
 - from surface only?
 - from crack tips only?
 - from existing cracks only?
- Constraints on turning angles?
- Constraints on crossing angles?
- Constraints on minimum fragment size?

Imagine 3D!





Have you ever seen a straight crack? smooth crack?



- Fracture is inherently a multi-scale phenomenon.
- Idealizing a material as homogeneous and isotropic is a vast idealization.
- Crack-front samples the subscale heterogeneity.
- Probability of seeing a straight crack propagate through a random field is zero.



Computational Approach

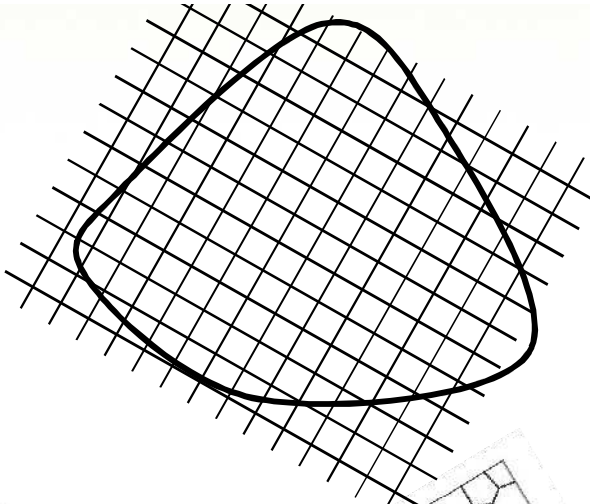
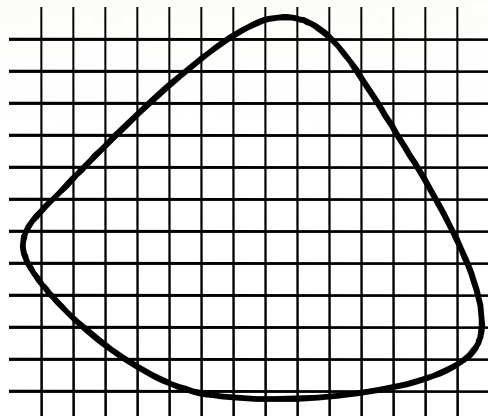
1. Random Voronoi tessellation (mesh)
2. Polyhedral finite-elements (shape functions generated by RKPM)
3. Fracture only allowed at element edges (dynamic change in mesh connectivity)
4. *Dynamic* insertion of cohesive tractions at limit surface
5. Penalty contact (discrete element paradigm)
6. Explicit dynamics solution

dynamic insertion of cohesive tractions based on . . .

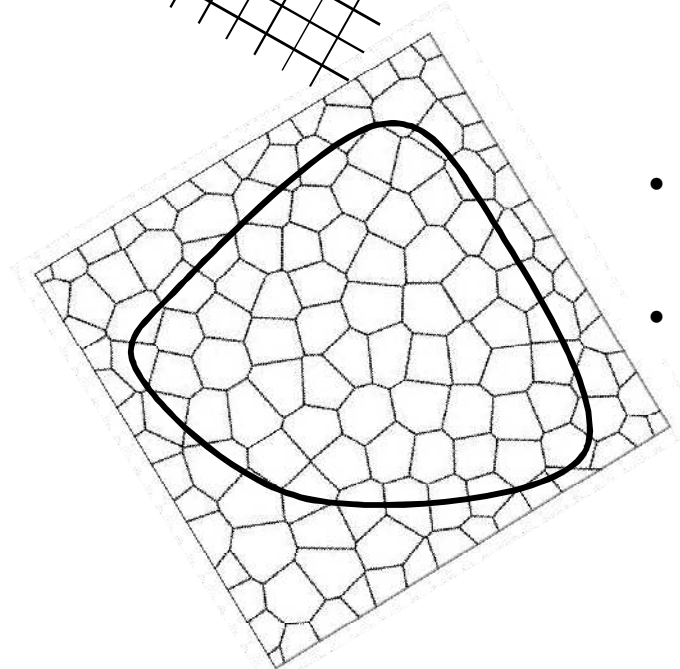
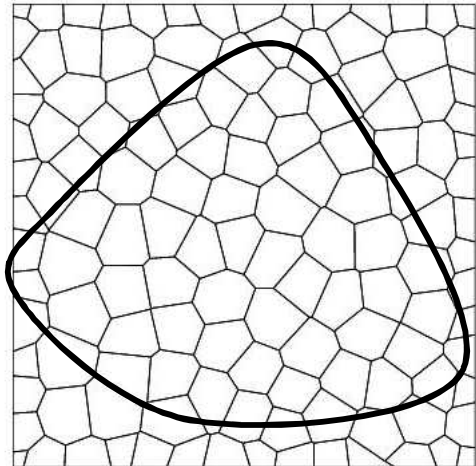
Pandolfi, A. and Ortiz, M. (2002) 'An efficient adaptive procedure for three-dimensional fragmentation simulations,' *Engineering with computers*, 18, 148-159.

Eliminating Mesh Induced Crack Bias

If cracks can grow only at element edges, then need to eliminate any directional bias in crack growth (well known in 'lattice' methods).



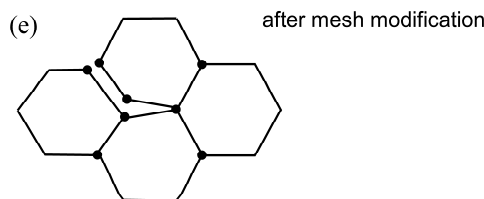
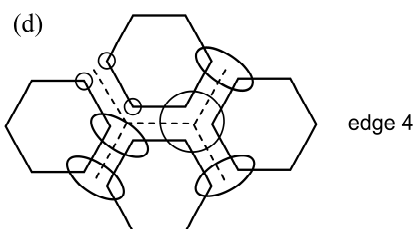
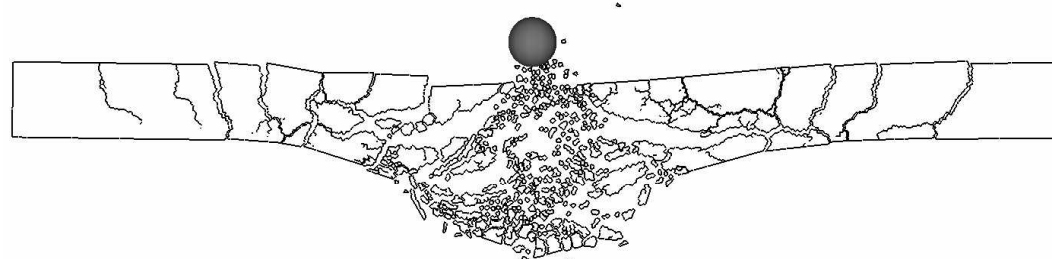
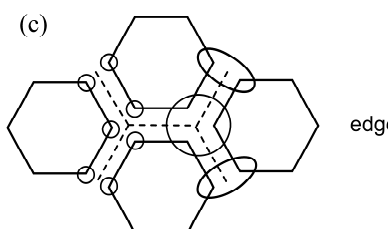
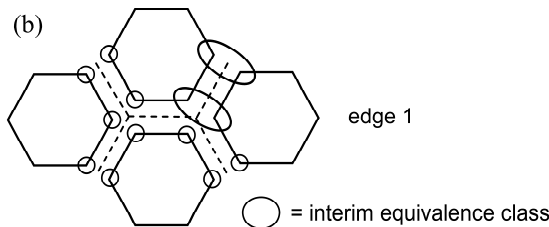
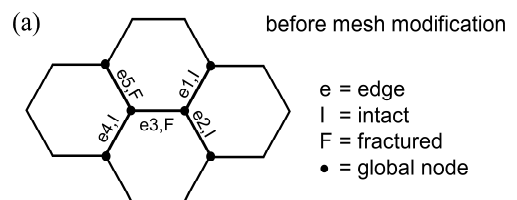
Structured grids can result in strong mesh induced bias (potentially nonobjective).



Voronoi tessellation of with random seeding

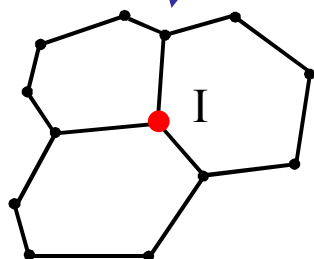
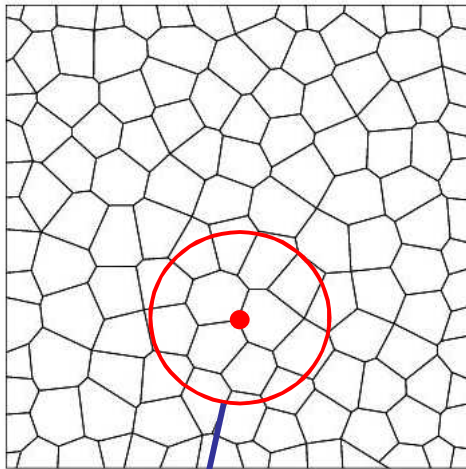
- need to use 'random' discretizations
- statistically isotropic

Dynamic Mesh Connectivity



Polyhedral Element Formulation

Use EFG/RKPM methodology to generate shape functions.

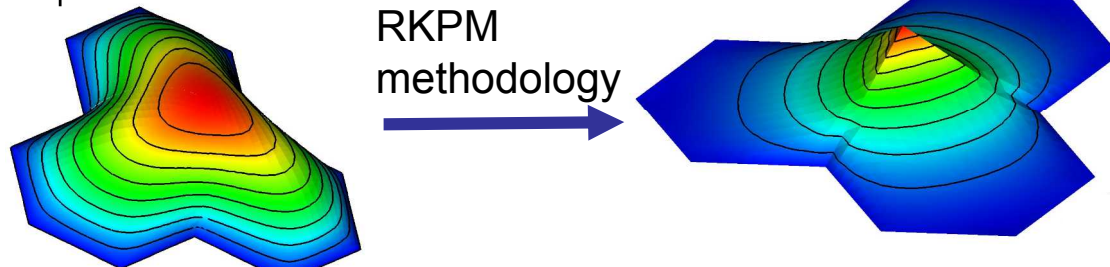


local support for node I

1. Generate nodal *weight* function ϕ by solving Poisson equation on compact support.
2. Generate nodal *shape* function ψ at each integration point using Reproducing Kernel Method.
3. Correct shape function derivatives to satisfy integration consistency (Gauss's theorem).

$$\nabla^2 \phi + 1 = 0$$

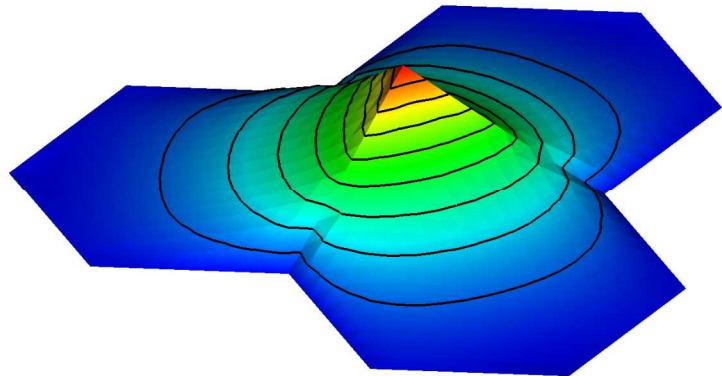
$$\phi = 0 \text{ on } \Gamma$$



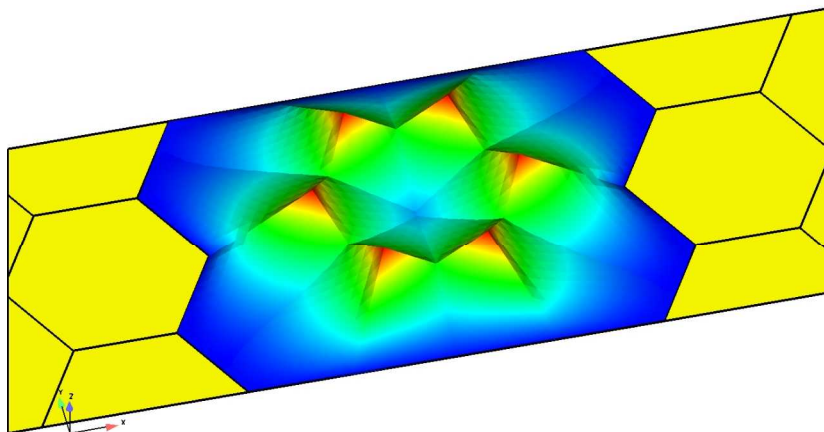
weight function ϕ

shape function ψ

Shape Function and Element Properties

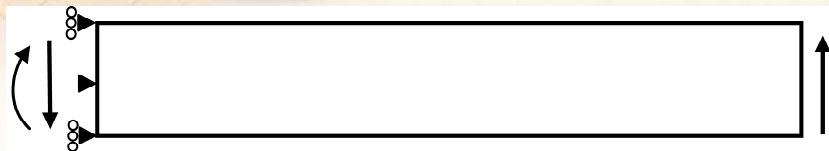


- partition of unity and x
- Kronecker delta property at nodes
- linear on edges
- works for non-convex elements
- shape functions defined on original configuration
- no mapping to 'parent' shape
- total-Lagrangian formulation
- mean-dilation formulation for incompressibility
- 'special' mass-lumping



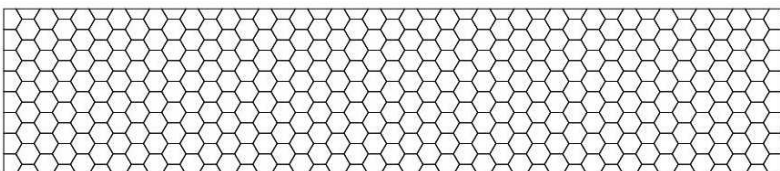
six nodal shape functions
for a regular hexagon

Effect of Shape for Hexagons

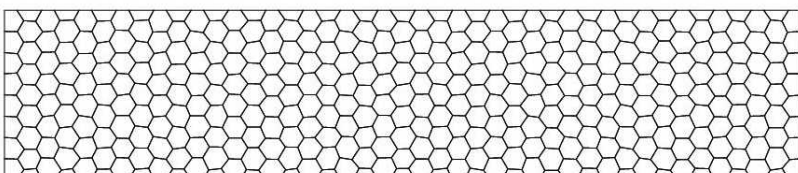


regular array of hexagons

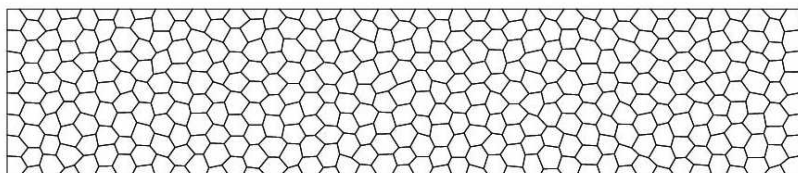
$r > 0 \Rightarrow$ random perturbation of node position



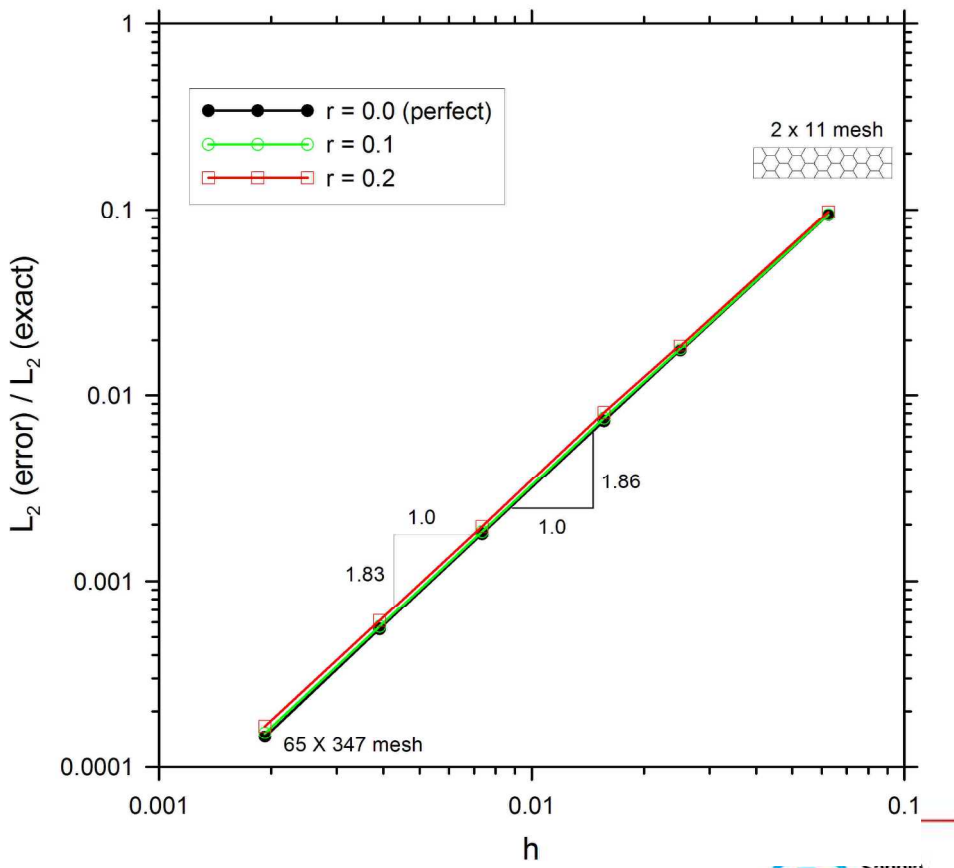
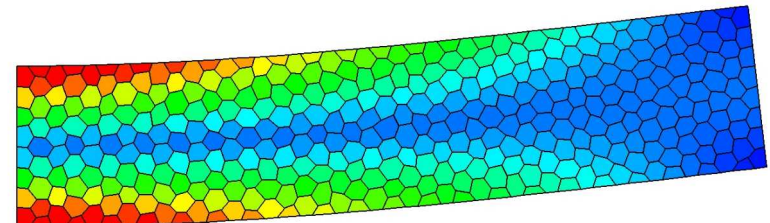
$r = 0.0$



$r = 0.1$

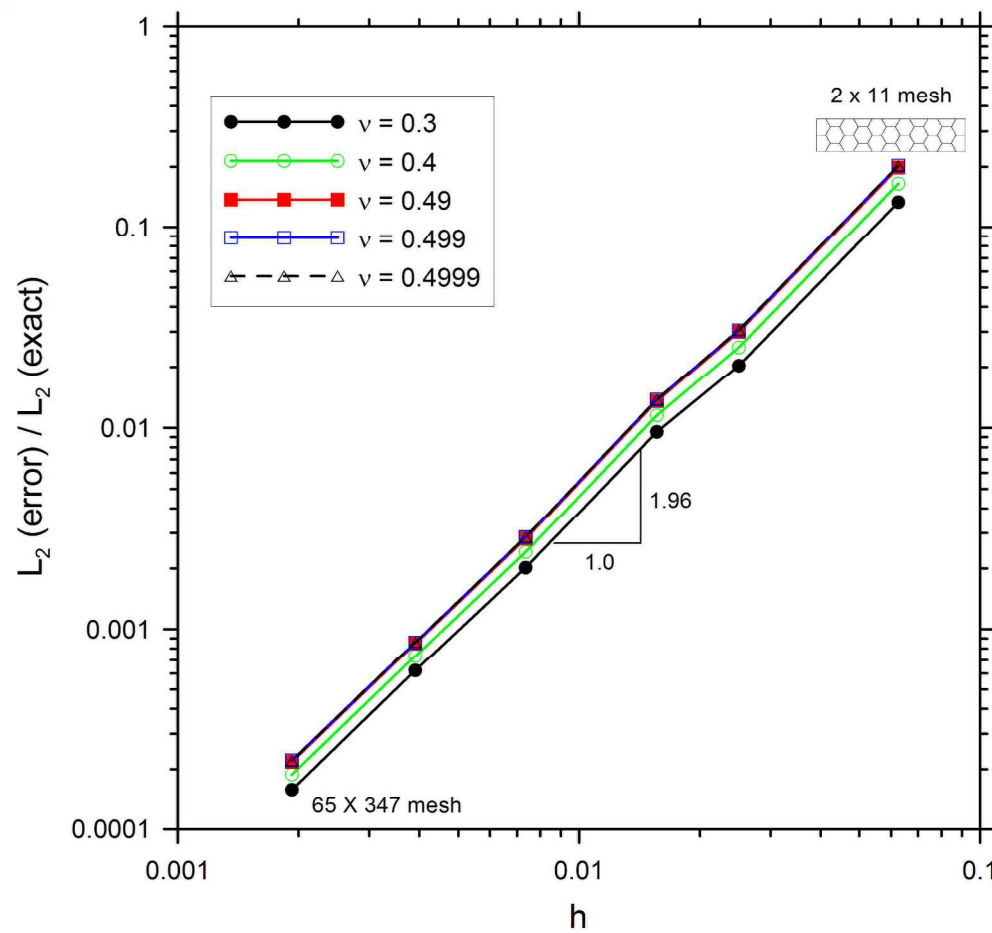


$r = 0.2$

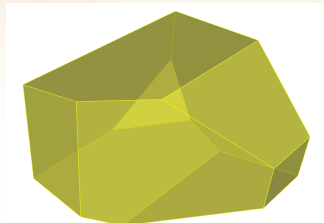


Mean Dilation Formulation

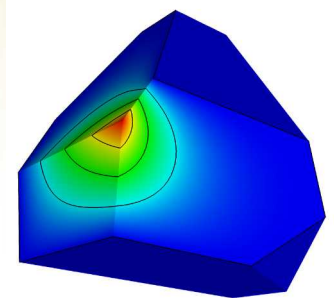
same as conventional FEM



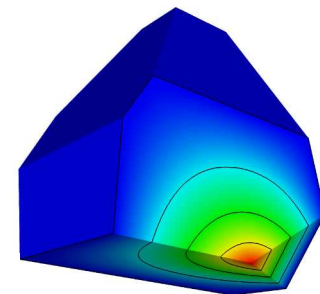
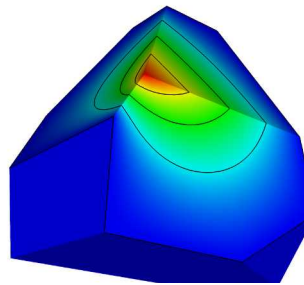
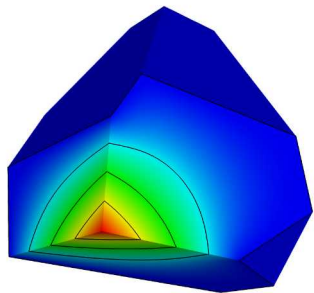
3D Arbitrary Polyhedral Element Formulation



polyhedral element



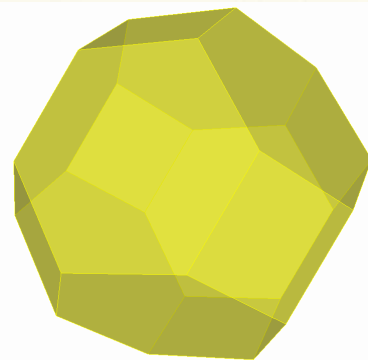
shape functions



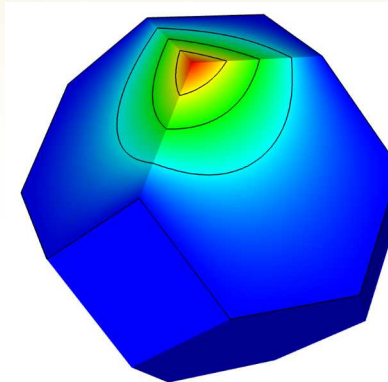
- arbitrary number of vertices and faces
- can have nonplanar faces
- works for non-convex elements
- uses harmonic shape functions (Joshi, 2007), defined on original configuration
- no isoparametric mapping to 'parent' shape
- need to use total-Lagrangian formulation
- number of integration points equals number of vertices (Rashid, 2006)
- partition of unity and \mathbf{x}
- Kronecker delta property at nodes
- compatible with existing finite elements
- mean dilation formulation for incompressibility



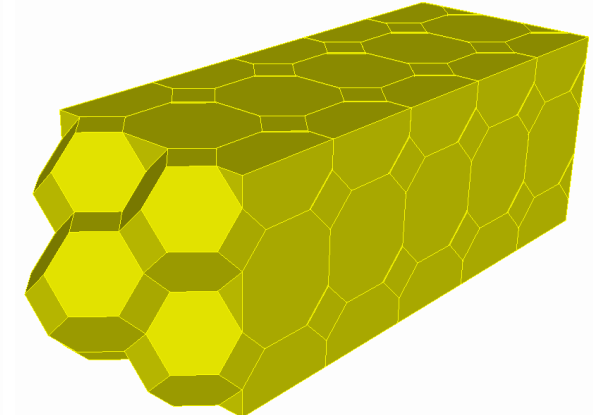
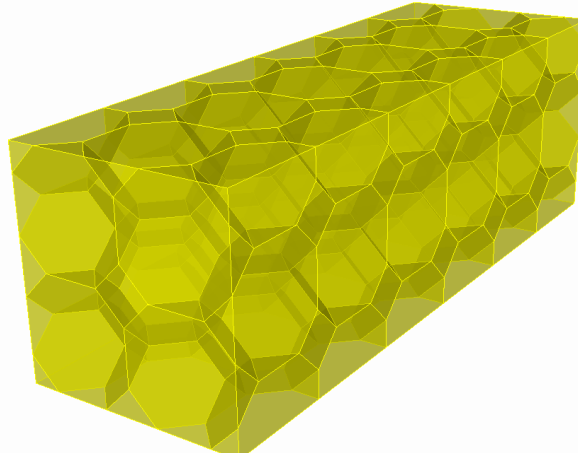
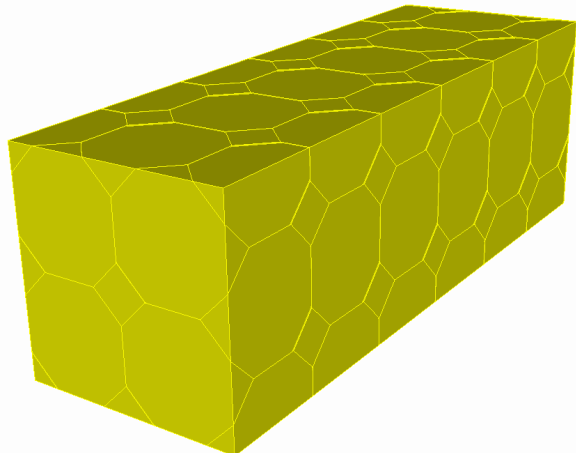
3D Verification



truncated octahedron

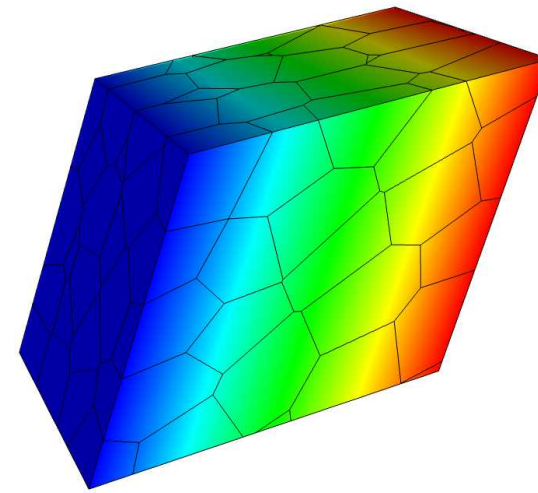
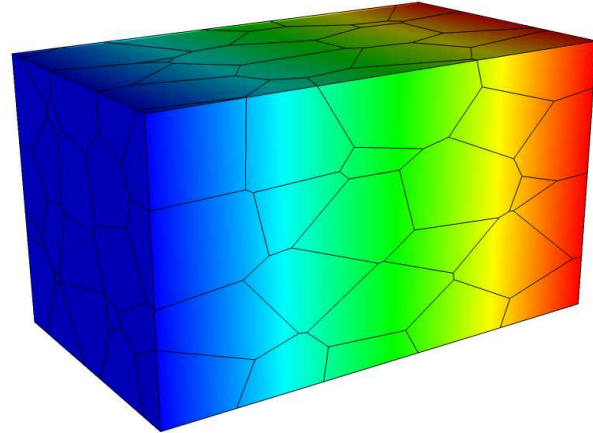
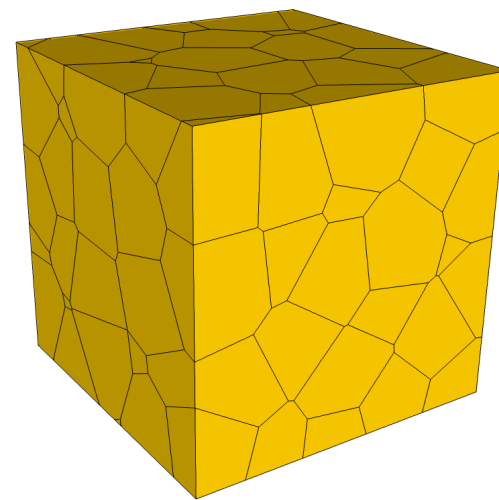


nodal shape function

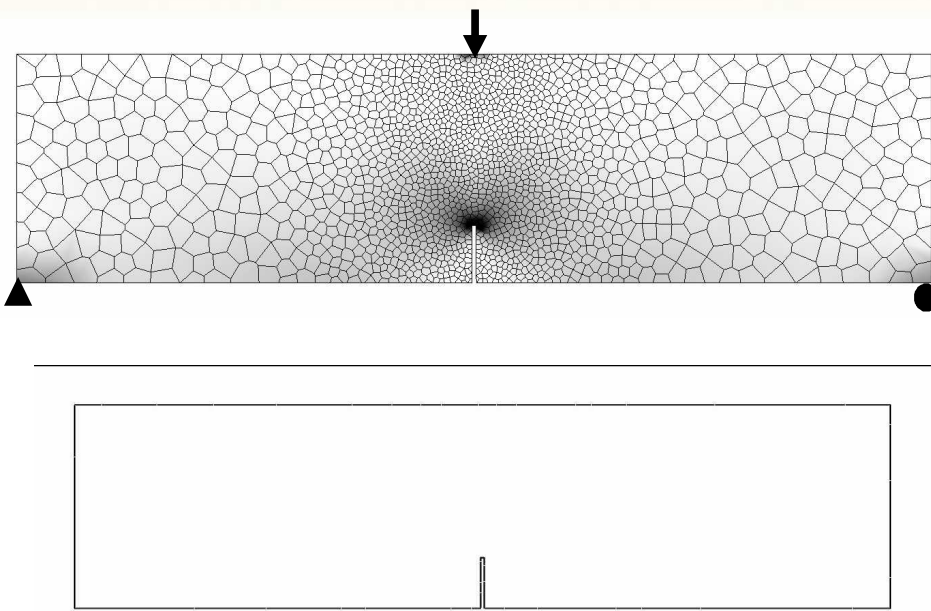




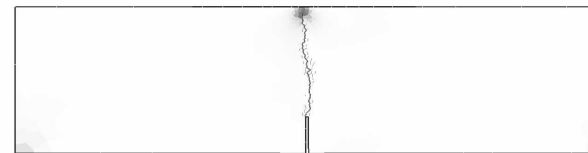
3D Verification



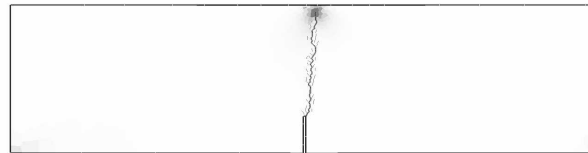
Example: 3pt-bend



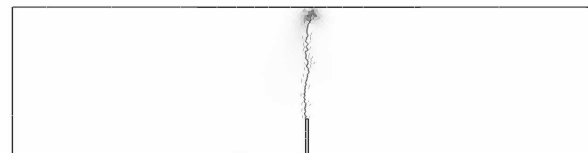
- quasistatic
- single crack growth



realization 1

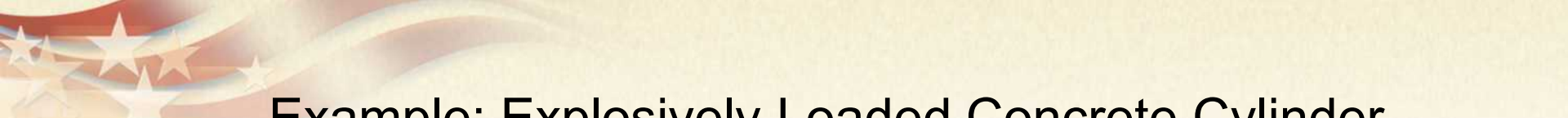


realization 2

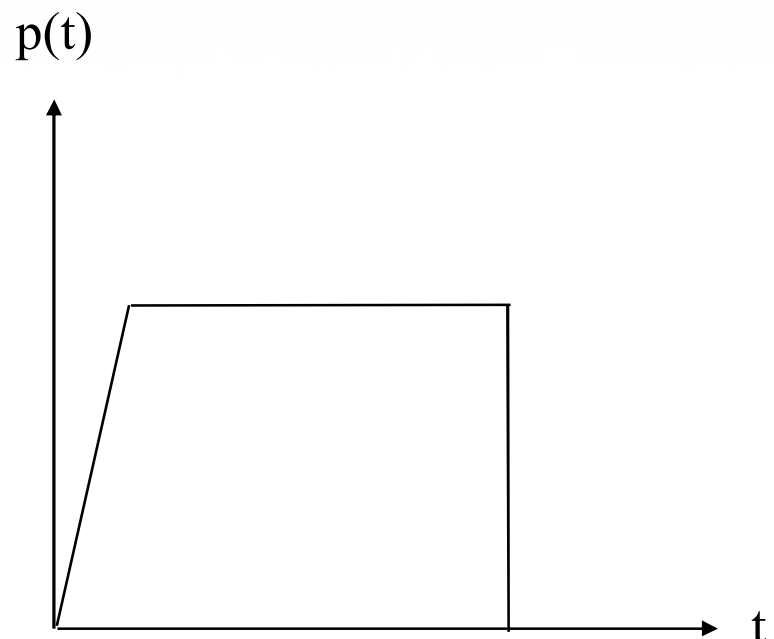
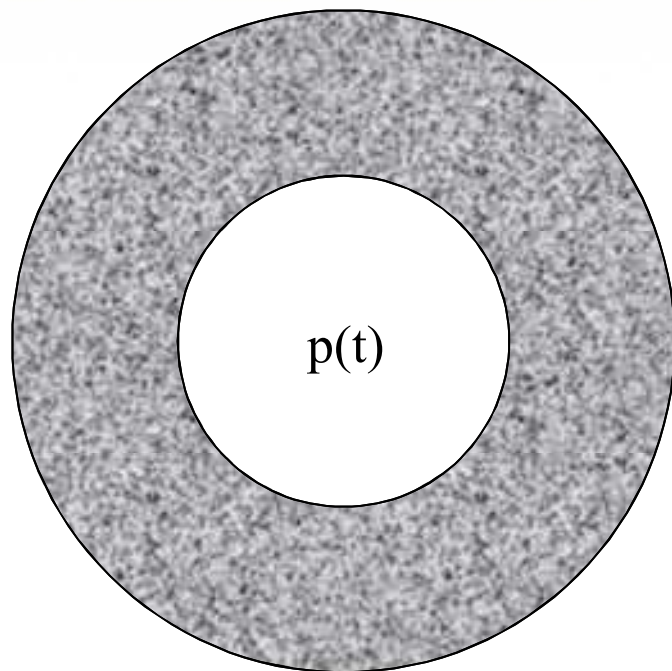


realization 3

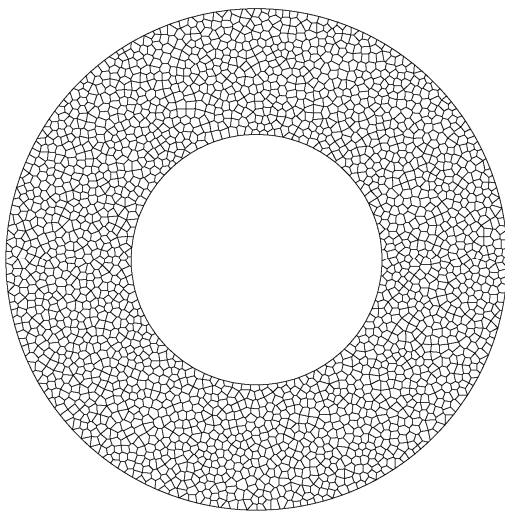
View mesh independence and convergence in terms of distributions of results.



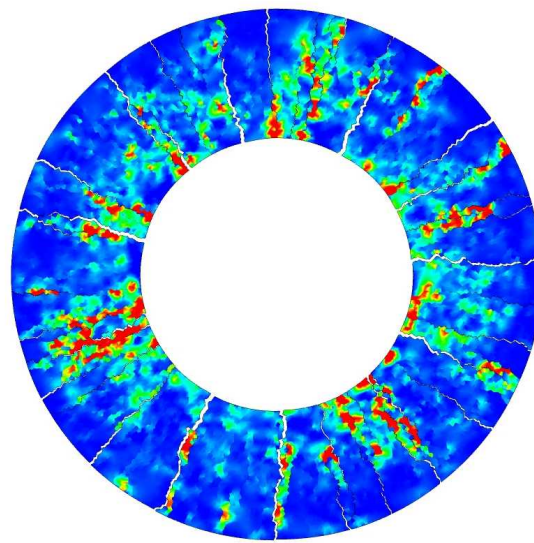
Example: Explosively Loaded Concrete Cylinder



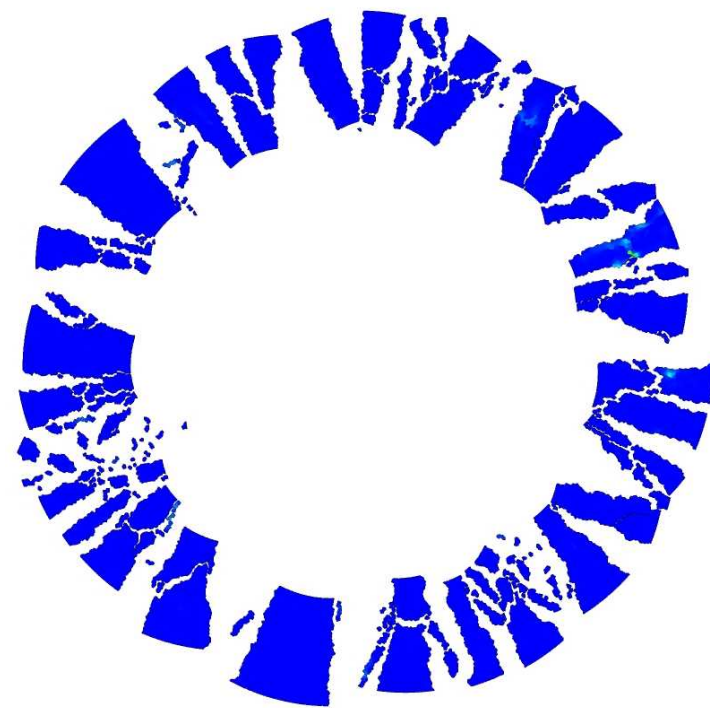
Example: Explosively Loaded Concrete Cylinder



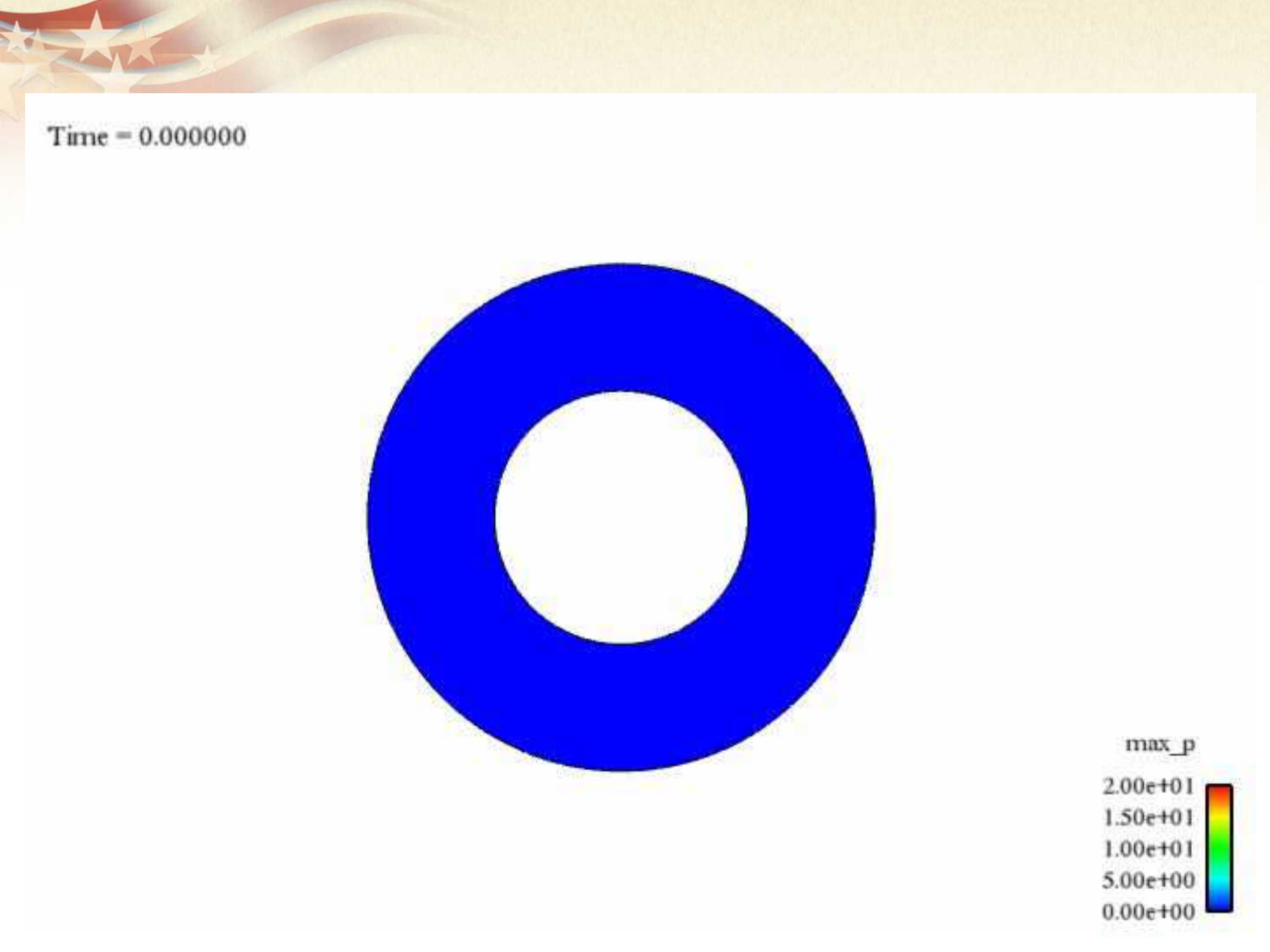
$t = 0$



$t = 2$ ms

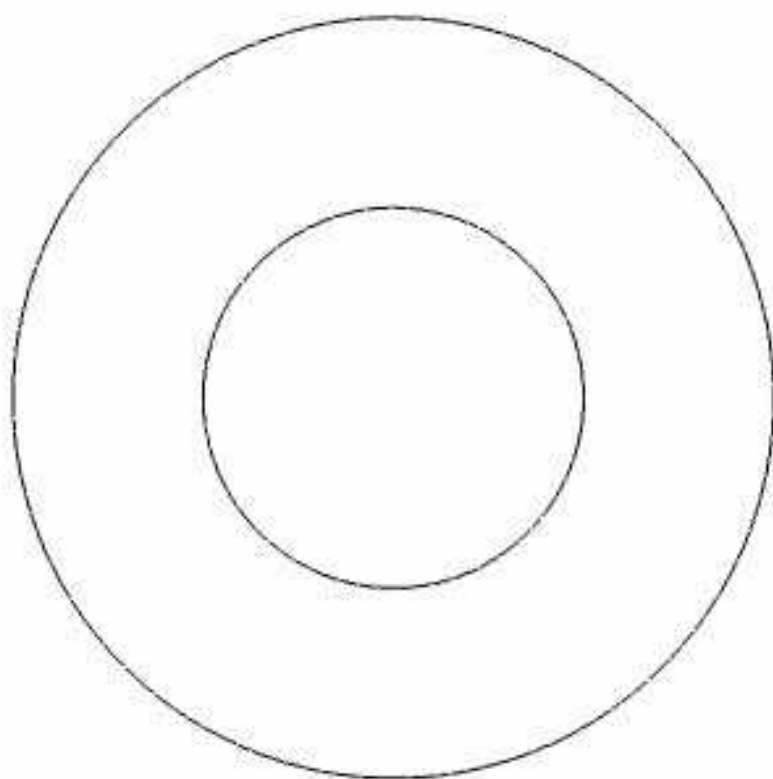


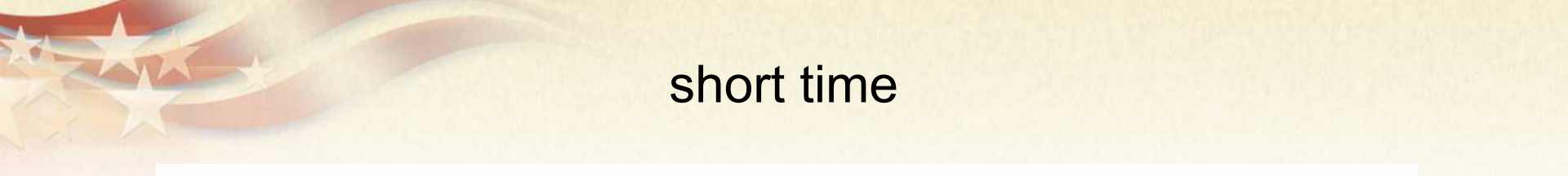
$t = 20$ ms





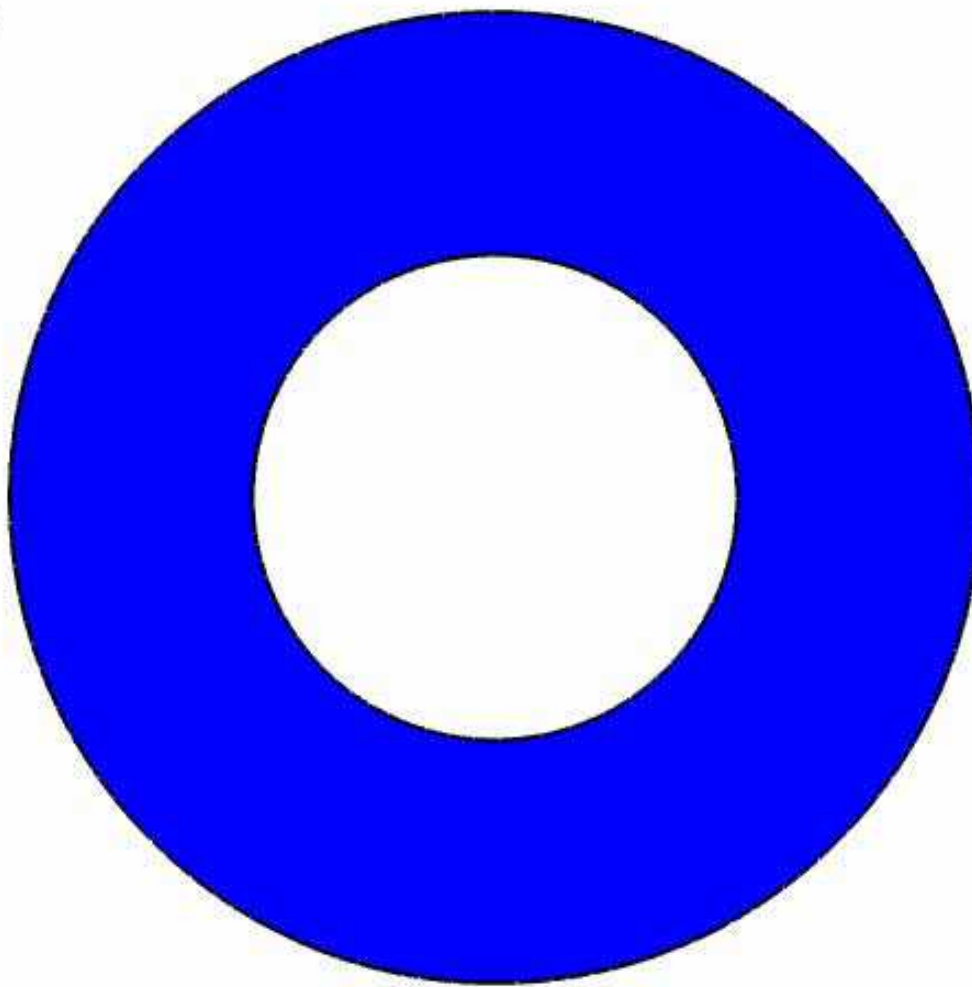
Time = 0.000000



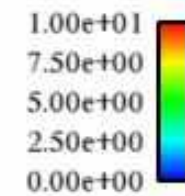


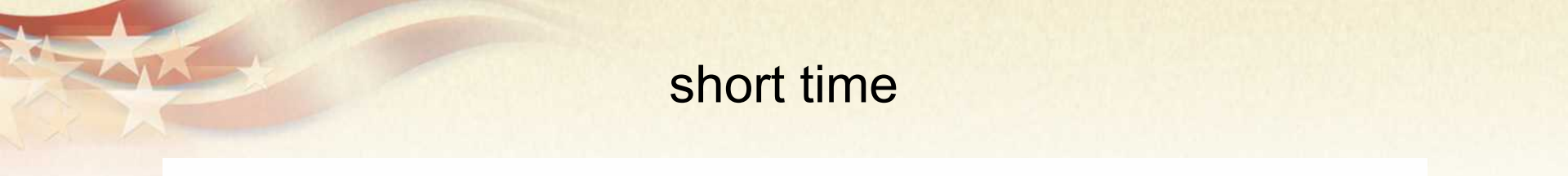
short time

Time = 0.000000



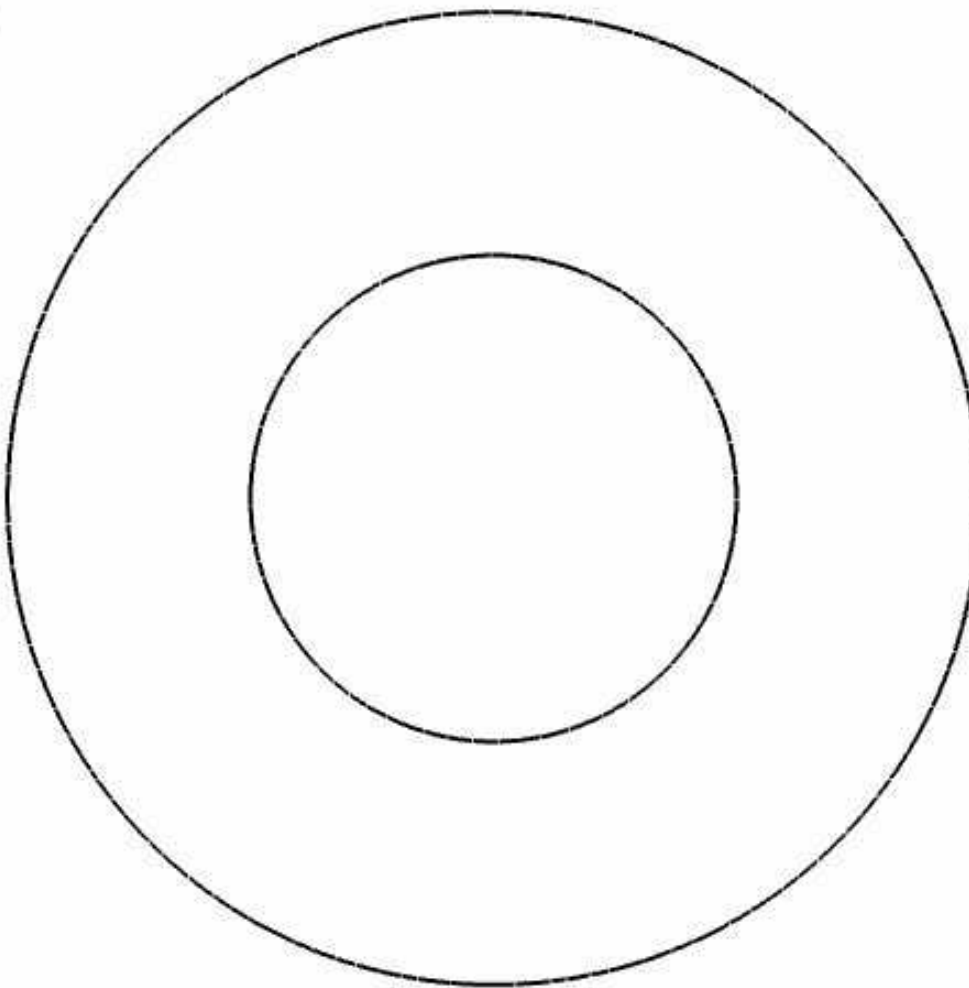
max_p





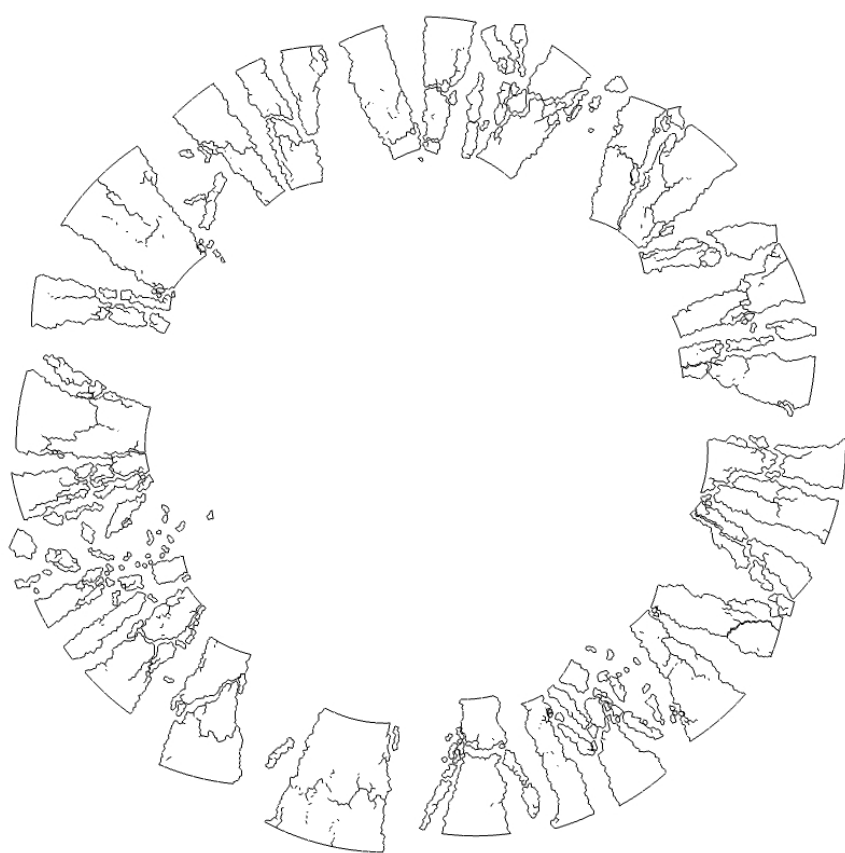
short time

Time = 0.000000



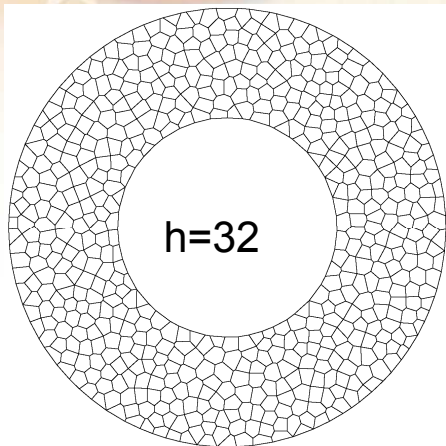


realization 1

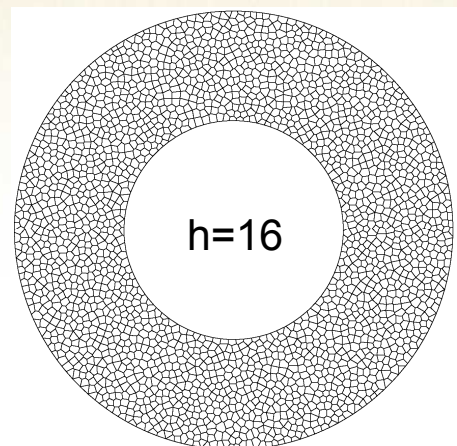


realization 2

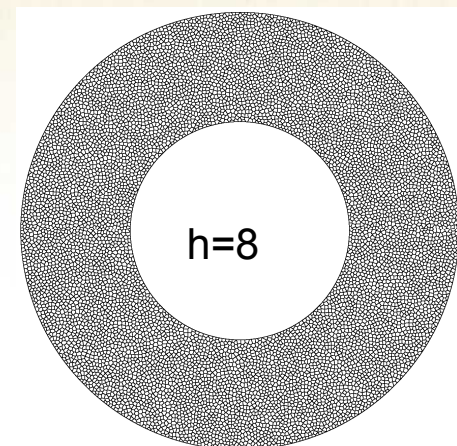




$h=32$



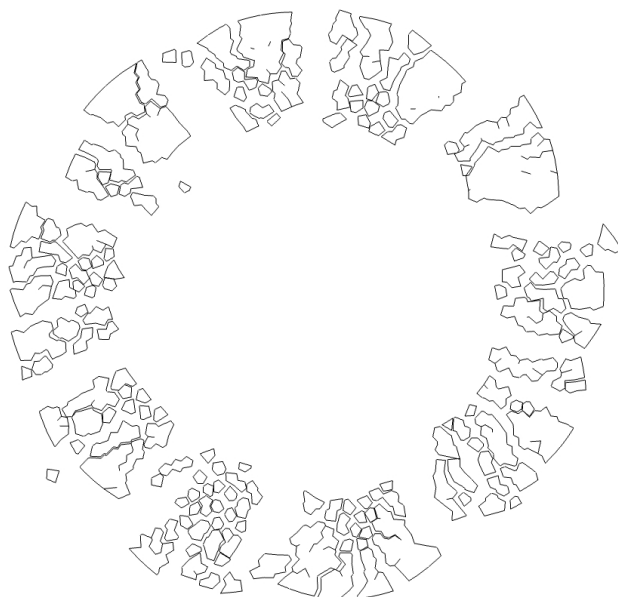
$h=16$



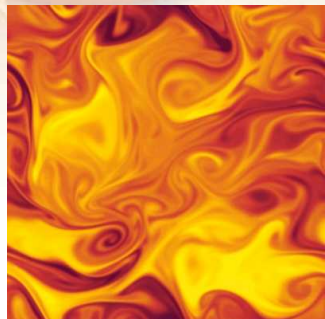
$h=8$



converging ?



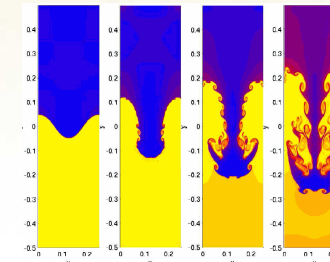
Nonlinear Dynamical Systems



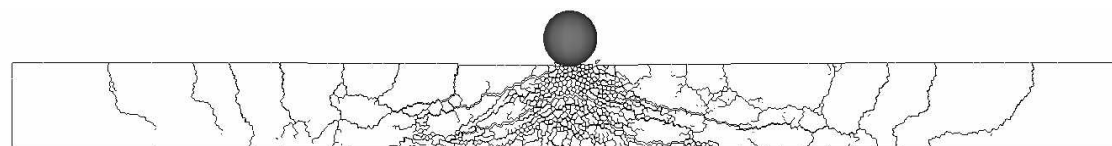
turbulence



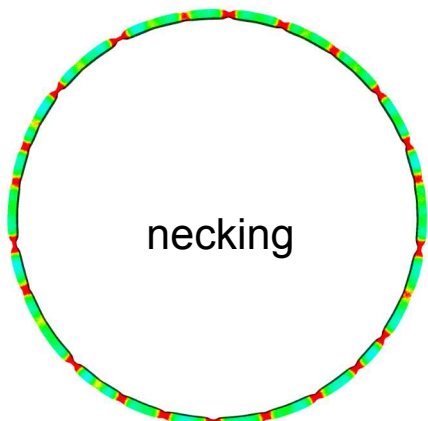
buckling



Rayleigh-Taylor instability



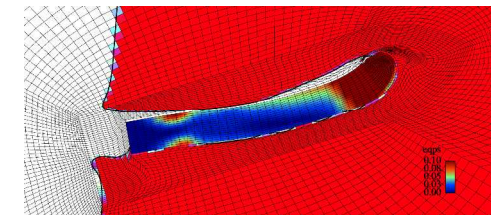
pervasive fracture



necking



shear banding



high speed penetration

- Exhibit extreme sensitivity to initial conditions and system parameters.
- Deterministic description is, in a sense, ill-posed.
- Regularize using a distributional description of inputs and outputs, e.g. (material variability, geometric variability).

Definitions of Statistical Convergence

$P_h(q)$ probability distribution for a given mesh resolution h

$F_h(q)$ cumulative distribution for a given mesh resolution h

q = engineering quantity of interest

Almost Sure Convergence

$$\lim_{h \rightarrow 0} P_h(q) = P(q) \quad \text{a.e.}$$

Convergence in r -mean

$$\lim_{h \rightarrow 0} E \left[|P_h(q) - P(q)|^r \right] = 0$$

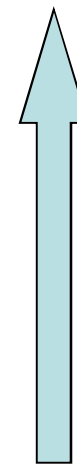
Convergence in Probability

$$\lim_{h \rightarrow 0} \Pr(P_h(q) - P(q) > \varepsilon) = 0$$

Convergence in Distribution

$$\lim_{h \rightarrow 0} F_h(q) = F(q)$$

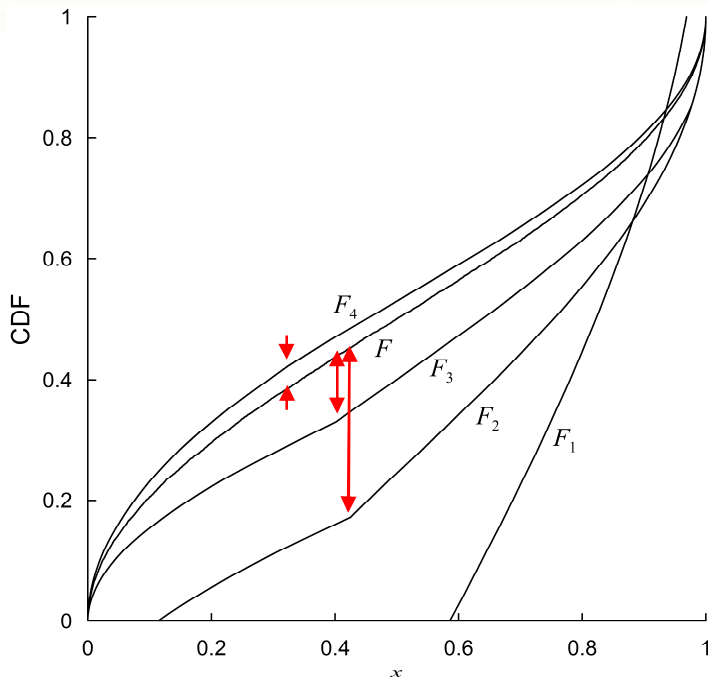
(Mode of convergence used to prove Central Limit Theorem.)



increasing strength

How to Assess Convergence in Distribution?

$$\lim_{h \rightarrow 0} F_h(q) = F(q)$$

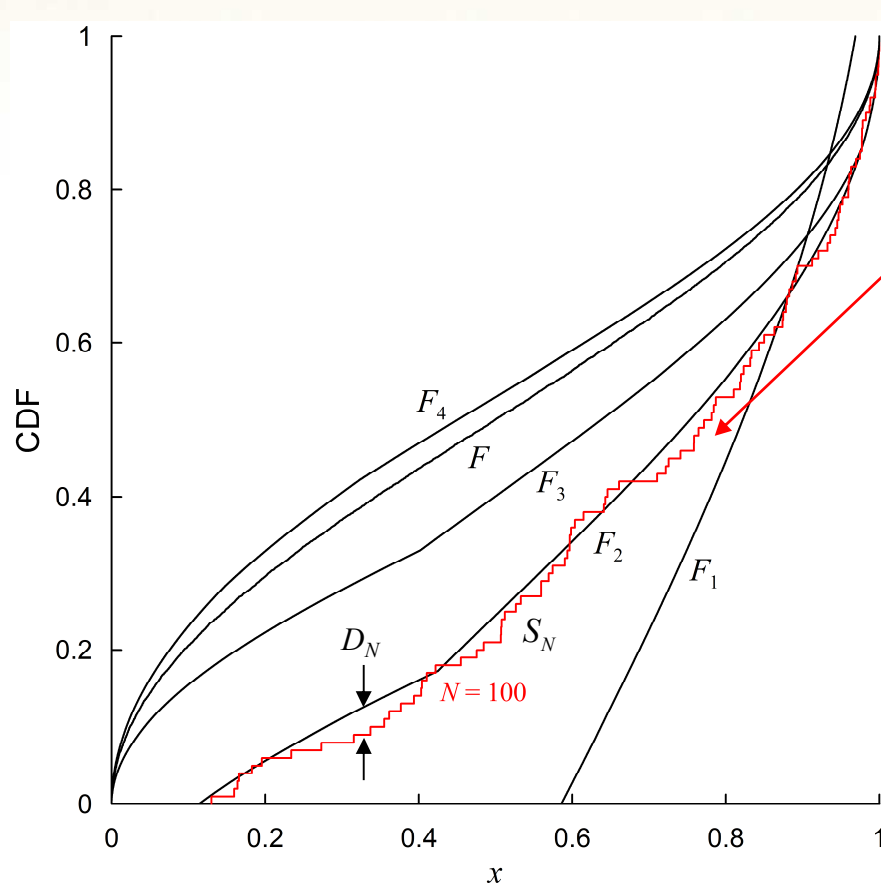


use L_∞ norm: $L_\infty(F_h, F) = \sup_x |F_h(x) - F(x)|$

To have a complete function space with this norm,
need to assume F_h is continuous.

(Space of continuous functions is complete in the L_∞ norm.)

What about finite sampling effects?



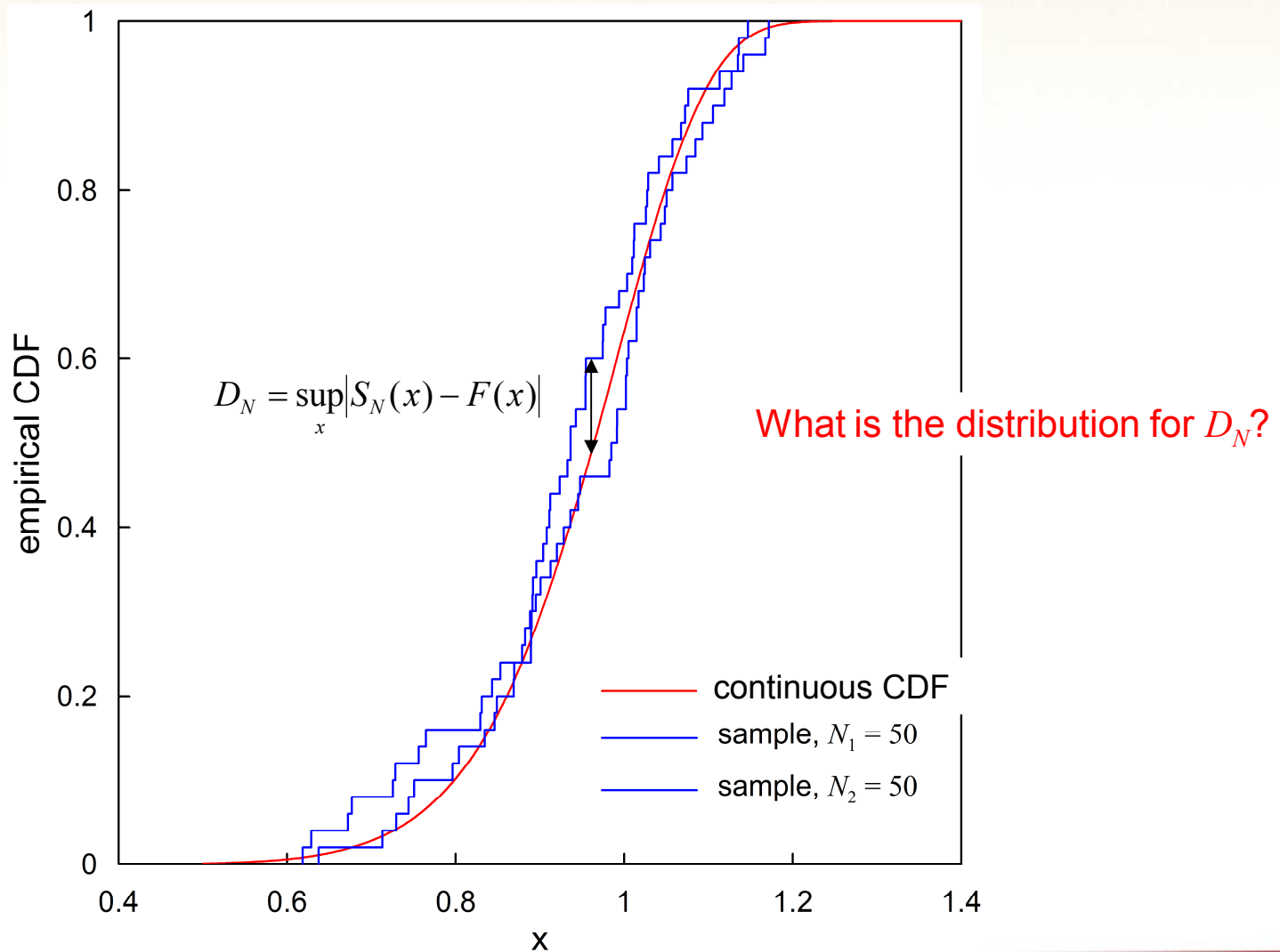
empirical CDF, $S_N(x)$

$$S_N(x) \equiv \begin{cases} 0, & x < x_1 \\ \frac{r}{N}, & x_r < x < x_{r+1} \quad r = 1, \dots, N-1 \\ 1, & x_N < x \end{cases}$$

Strong Law of Large Numbers:

$$\lim_{N \rightarrow \infty} S_N(x) = F(x) \text{ (almost surely)}$$

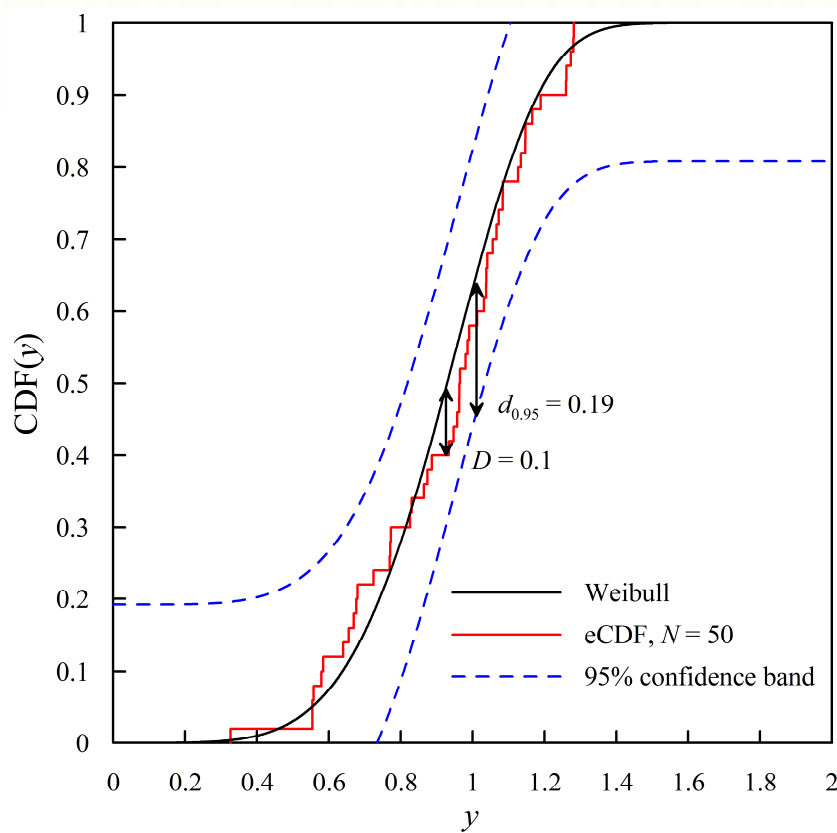
Kolmogorov-Smirnov Statistic



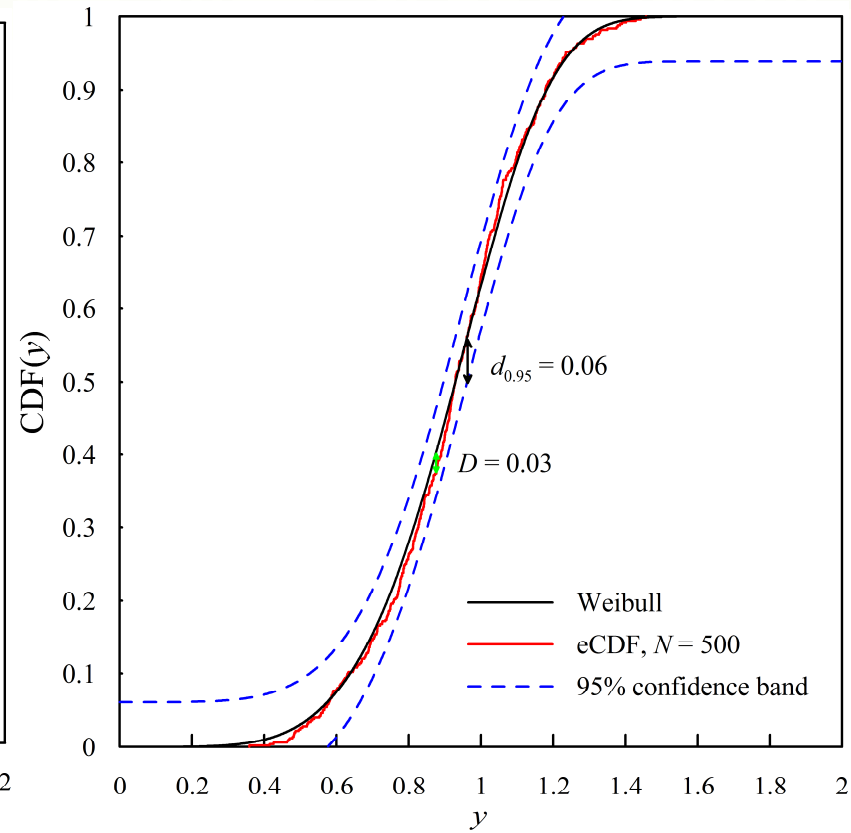
Kolmogorov-Smirnov Statistic

95% confidence bounds

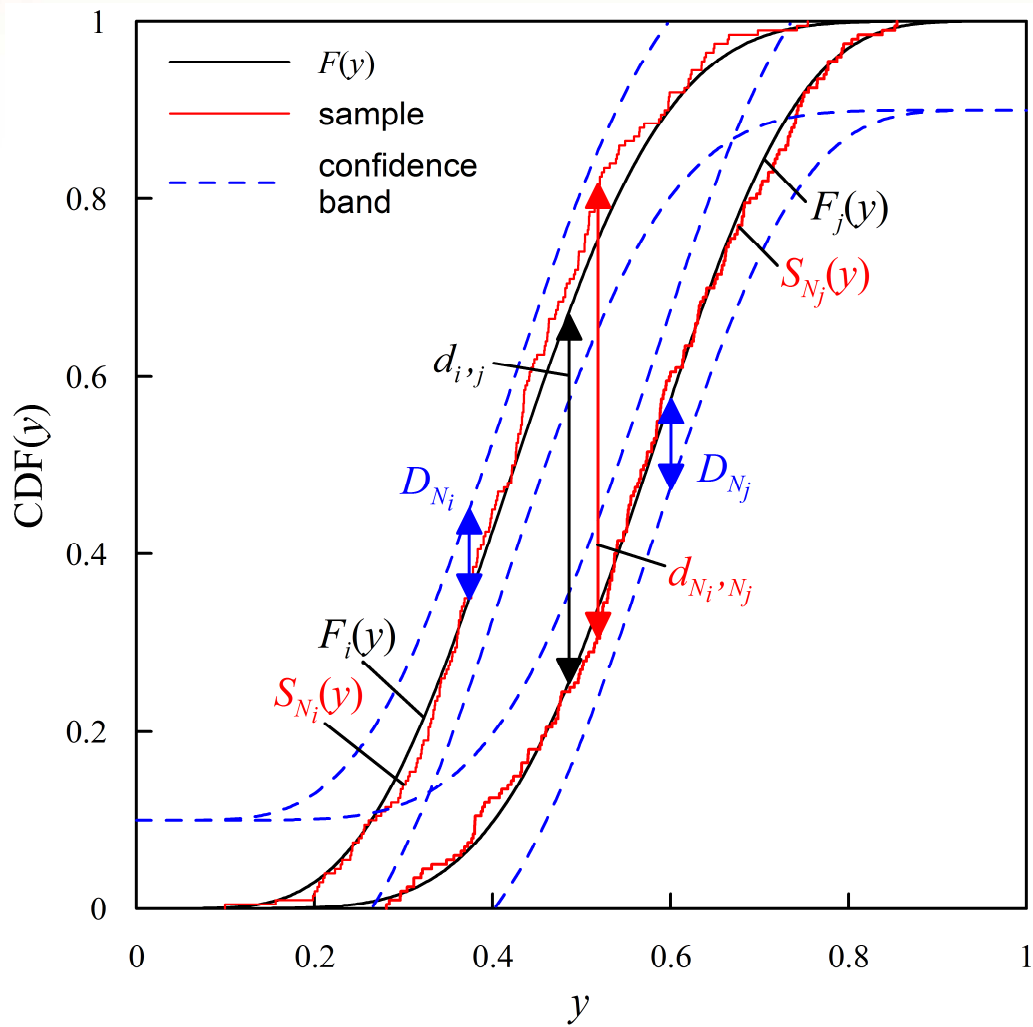
$N = 50$



$N = 500$



How to use KS-statistic to assess convergence-in-distribution with finite sample sizes?



$$|d_{i,j} - d_{N_i, N_j}| \leq D_{N_i} + D_{N_j} = \frac{z_i}{\sqrt{N_i}} + \frac{z_j}{\sqrt{N_j}}$$

Also, joint probability reduces confidence level.

Example: Ductile Thin Ring Expansion

Grady, D. and D. Benson (1983). "Fragmentation of metal rings by electromagnetic loading." *Experimental Mechanics* 23(4): 393-400.

Fragmentation of Metal Rings by Electromagnetic Loading

Fragmentation studies on rapidly expanding metal rings are performed with electromagnetic loading. Dynamic-fracture strain and fragment-size measurements are reported for aluminum and copper

by D.E. Grady and D.A. Benson

ABSTRACT—A method is described for performing fragmentation studies on rapidly expanding metal rings. A fast-discharge capacitor system generates magnetic forces which accelerate the rings to maximum radial velocities of approximately 200 m/s corresponding to circumferential-strain rates of approximately $10^7/s$ at fragmentation. Streak-camera techniques are used to record the time-resolved motion of the rings. Fracture-strain and fragmentation experiments have been performed on samples of OFHC copper and 1100-O aluminum.

Introduction

The fragmentation of a body due to a violent impulsive load is a complicated phenomenon which currently cannot be calculated with confidence. Dynamic loading leads to myriad interactions of stress waves which govern the fragmentation event. In addition, material-property effects and statistics of the fracture nucleation and growth process are also important.

Interpretation of dynamic-fracture experiments is complicated by the multiaxial and heterogeneous stress states occurring in most impact- or explosive-loading studies. Consequently, experimental methods which simplify the stress conditions leading to fragmentation of the body offer a better possibility of understanding the principles governing dynamic fragmentation. One attractive method is provided by radial loading of ring-shape specimens with magnetic forces in which dynamic fracture and fragmentation is brought about by the rapid application of a homogeneous one-dimensional tensile stress. The present report describes such radial-loading fragmentation experiments. Data on ring samples of 1100-O aluminum and OFHC copper are also provided.

The expansion of rings and cylindrical shells has been used productively in the past to investigate the phenomena of dynamic deformation. Numerous studies by direct application of explosive loading to the interior wall of cylindrical samples have been made. The method is extremely energetic, however. Experimental control is

complicated by the explosive violence, product gases, and preconditioning of samples through application of the initial high-amplitude shock wave. An improved laboratory technique has been explored¹ where the sample ring is isolated from the explosive by a cylindrical, high-strength metal mandrel. Recently, Warnes *et al.*² have extended this technique and used velocity interferometry to determine time-resolved motion of the expanding ring. Again, there is concern about shock preconditioning of the sample. Shock-wave studies indicate that material properties in metals can be severely altered by shock stresses above approximately 10 GPa.^{3,4} Also, the impulse provided by this method is not sufficient to produce significant fragmentation.

The application of magnetic forces to load ring or cylindrical geometries appears to have been described in the literature first by Niordson.⁵ A similar system has been described by Walling and Forrestal⁶ and used by Wesenberg and Sagartz⁷ to conduct fragmentation studies on large aluminum cylinders, illustrating the energy capability of this technique. Magnetic loading has several attractive features: (1) motion is imparted to the sample through continuous body forces rather than shock loading and consequently, preconditioning shock effects are eliminated; (2) loading rates are readily controlled through variation in rate and amplitude of the driving-current pulse; and (3) the method is more conducive to a laboratory environment than explosive-loading schemes. A magnetic-loading technique is not without its drawbacks, however. Since it is based on the principle of opposing forces between primary and induced currents, inductive heating, which may also have preconditioning effects, can occur in the sample material. Also, when fragmentation occurs, arcing of induced currents can result in additional local-heating effects.

The system that we have developed to conduct fragmentation experiments on metal rings is modest compared to the 250-kJ fast-discharge capacitor system described by Walling and Forrestal.⁶ The present method uses approximately 10 kJ of energy and compares most closely to the work described by Niordson.⁵ Implementation of the technique required additional development, however, and consequently, some description is warranted. For example, smaller experimental assemblies were found to be more sensitive to loading instabilities and different techniques were needed to apply the magnetic forces. The method

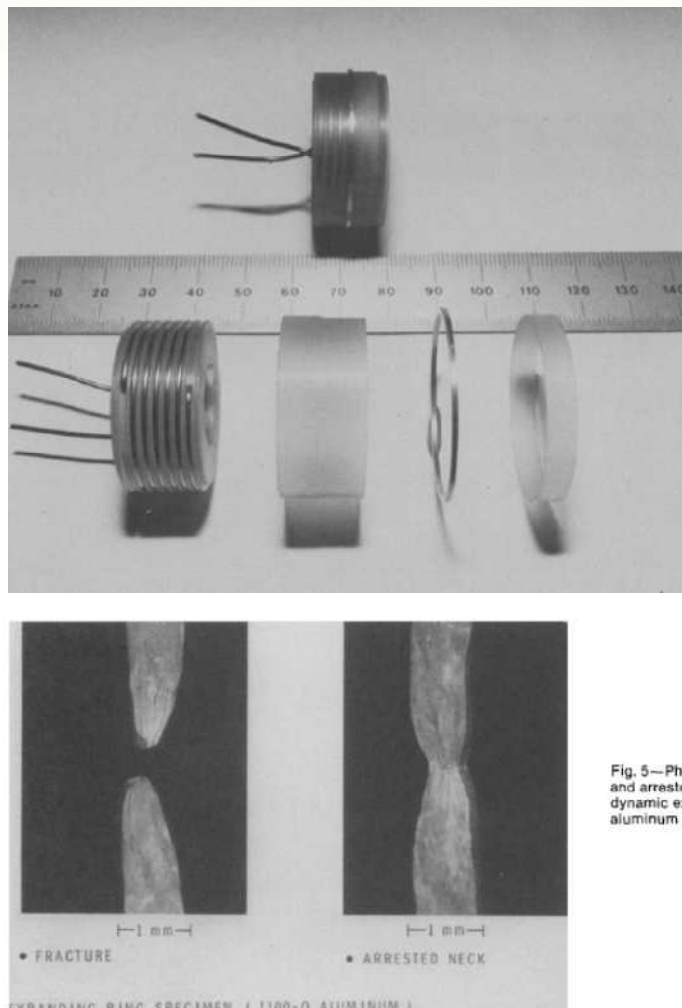
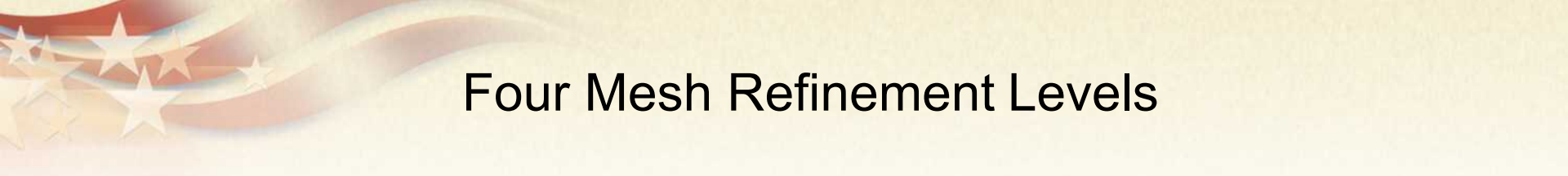


Fig. 5—Photograph of fracture and arrested-neck region from dynamic expansion of an aluminum ring

D.E. Grady and D.A. Benson are Research Scientists, Sandia National Laboratories, Albuquerque, NM 87185.

Original manuscript submitted: March 29, 1982. Final version received: July 11, 1983.



Four Mesh Refinement Levels

R0

- 6K elements
- 1 proc. on workstation
- ~10 min runtime

R1

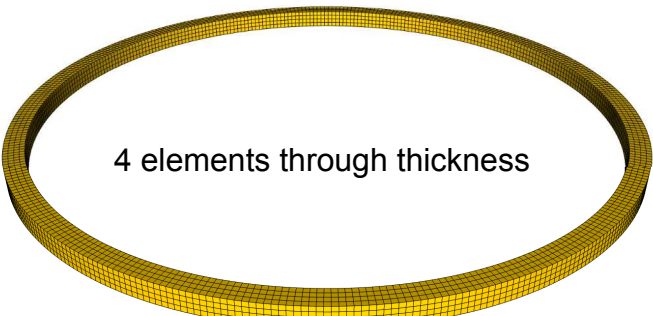
- 48K elements
- 1 proc. on workstation
- ~2 hour runtime

R2

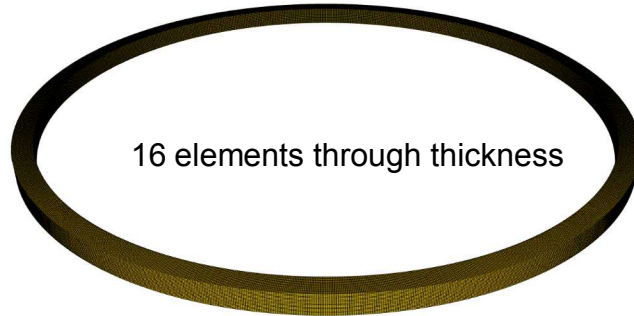
- 385K elements
- 16 proc. on tbird
- ~2 hour runtime

R3

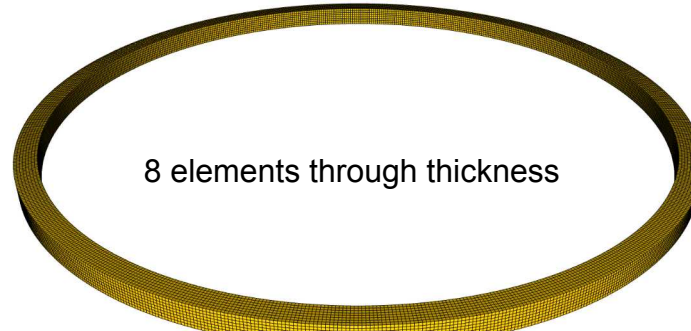
- 3M elements
- 128 proc. on tbird
- ~4 hour runtime



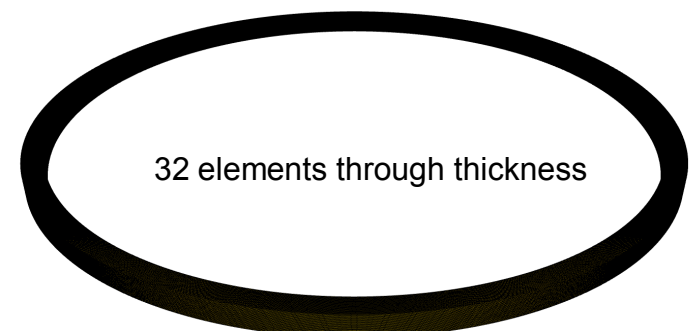
4 elements through thickness



16 elements through thickness



8 elements through thickness

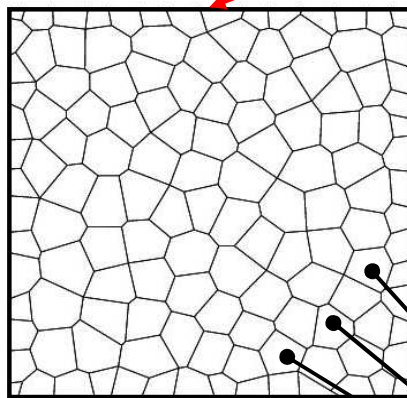


32 elements through thickness

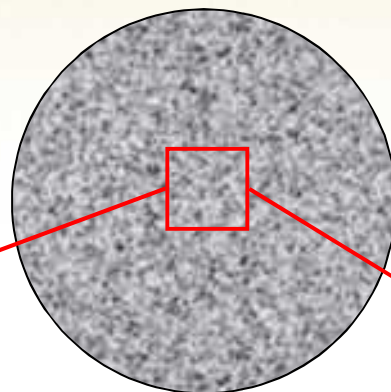
Approaches to Material Texture

Voronoi texture

model material variability via a Voronoi texture



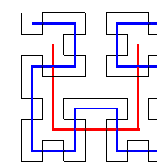
currently in EMU
(Stewart Silling)



Hilbert texture

model material variability via a Hilbert texture

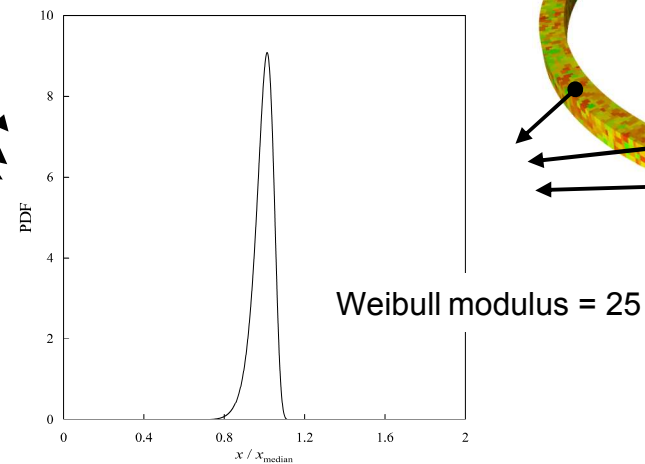
Hilbert space filling curve



2D

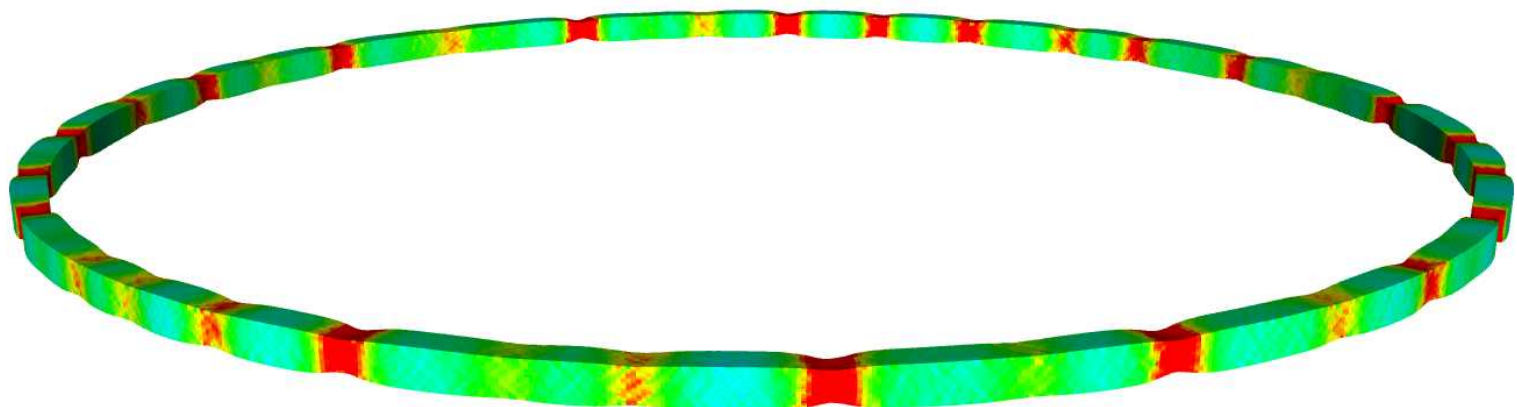
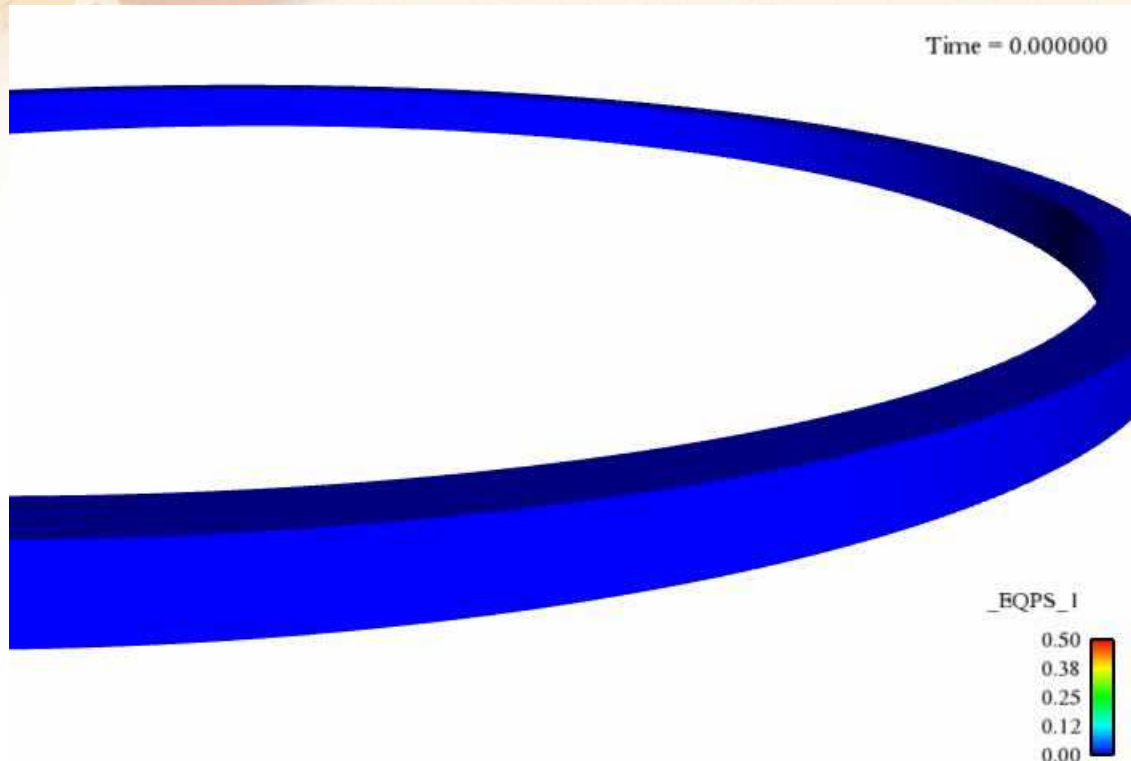
3D

Weibull Probability Density

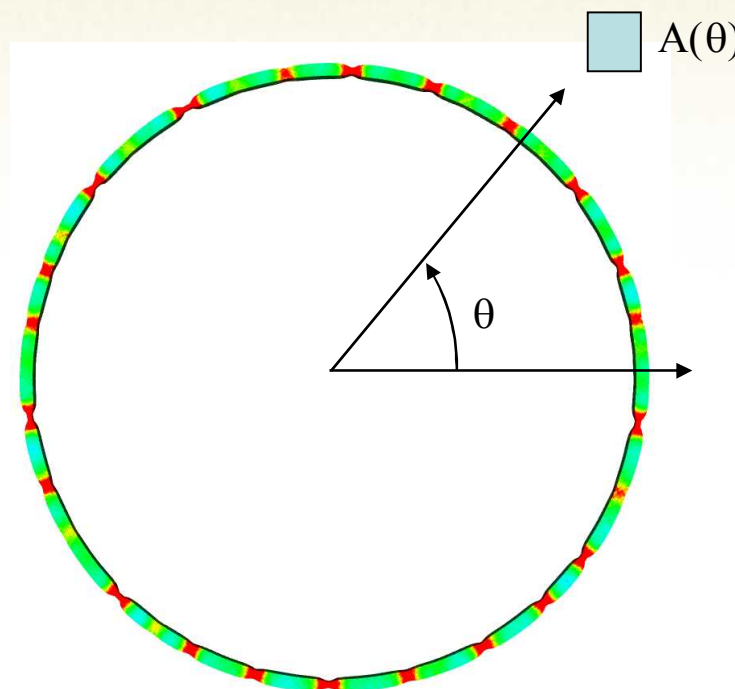


currently in Alegra
(Allen Robinson)

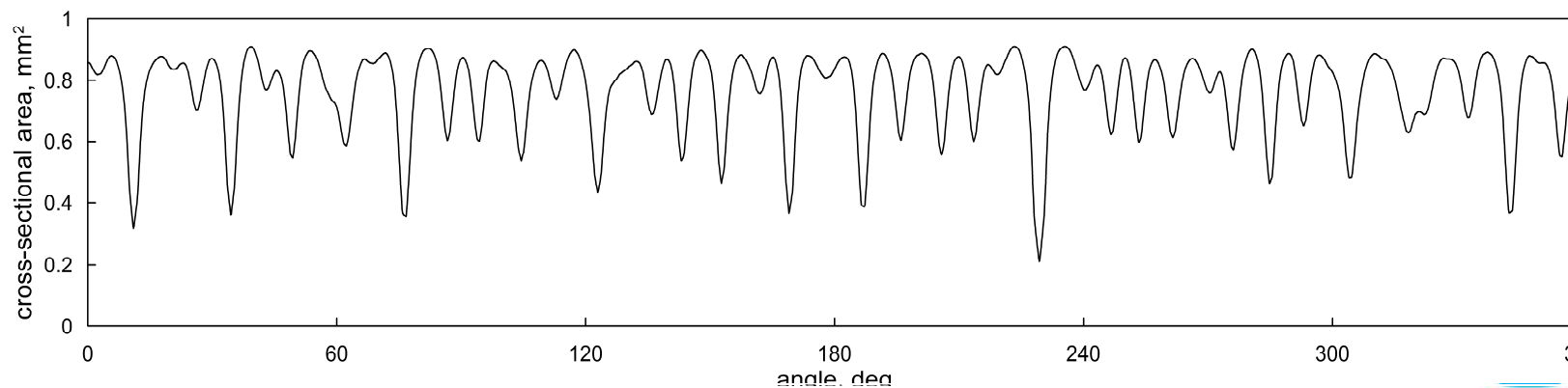
Simulation



Cross-Sectional Area

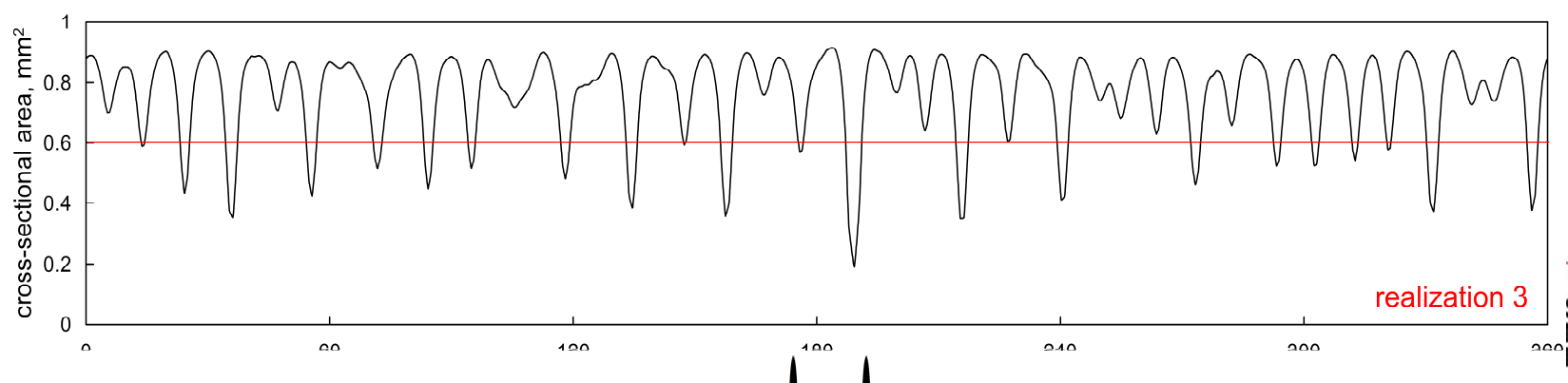
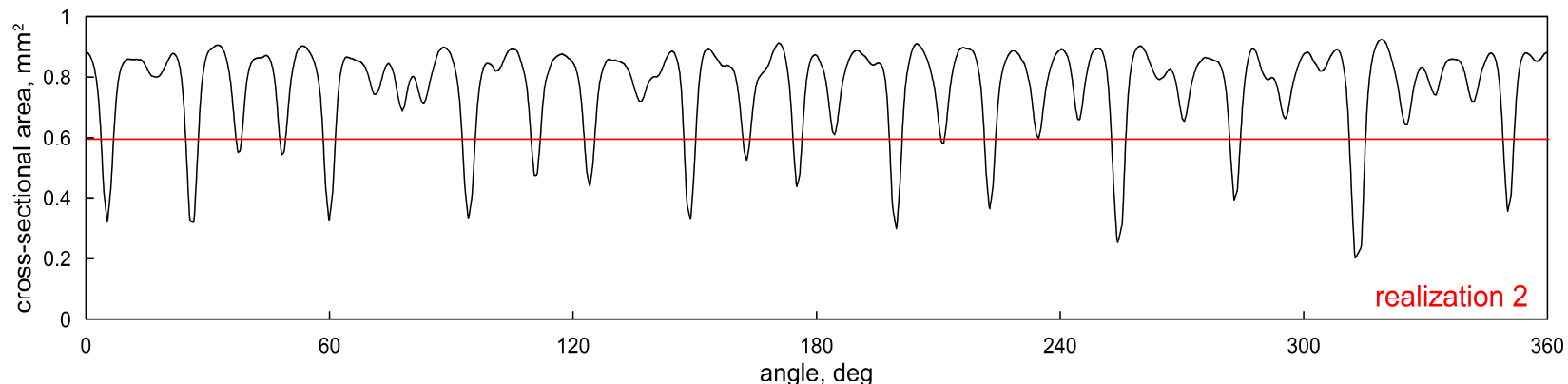
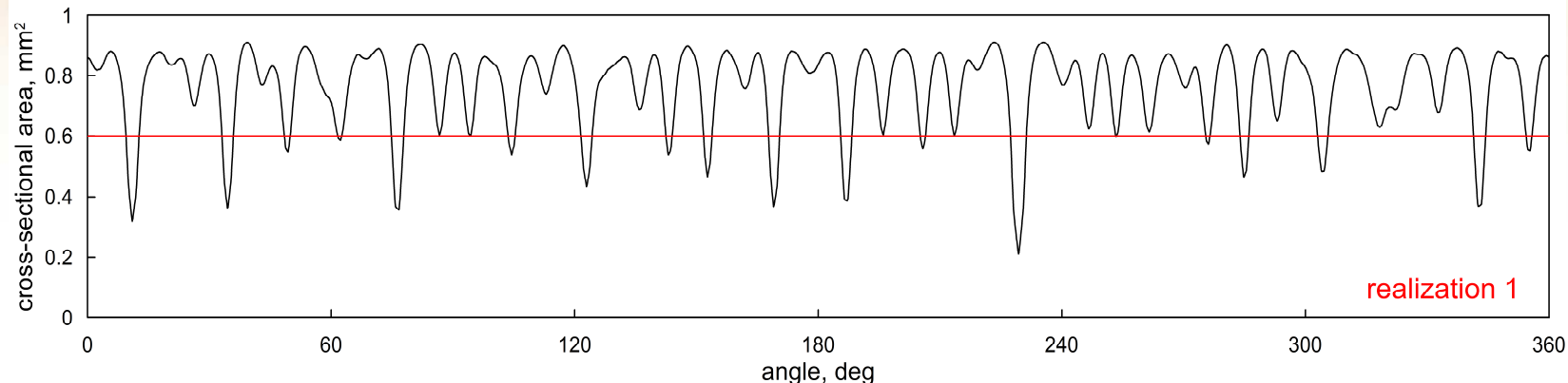


Reduce 3D random field to 1D random field.

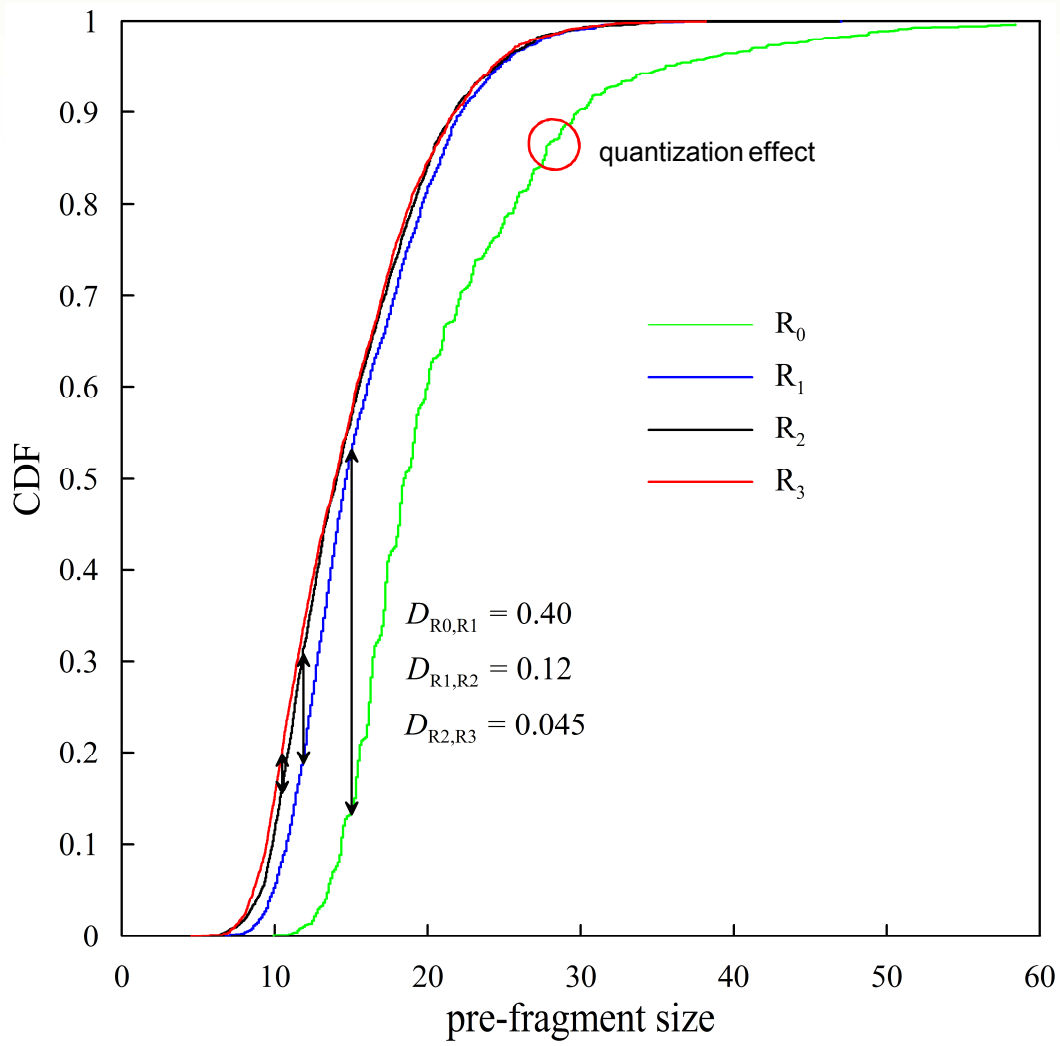


Neck Identification

ring cross sectional area at time = $40\mu\text{s}$, mesh refinement 1



Convergence in Distribution? with material texture



100 run ensemble

sample sizes

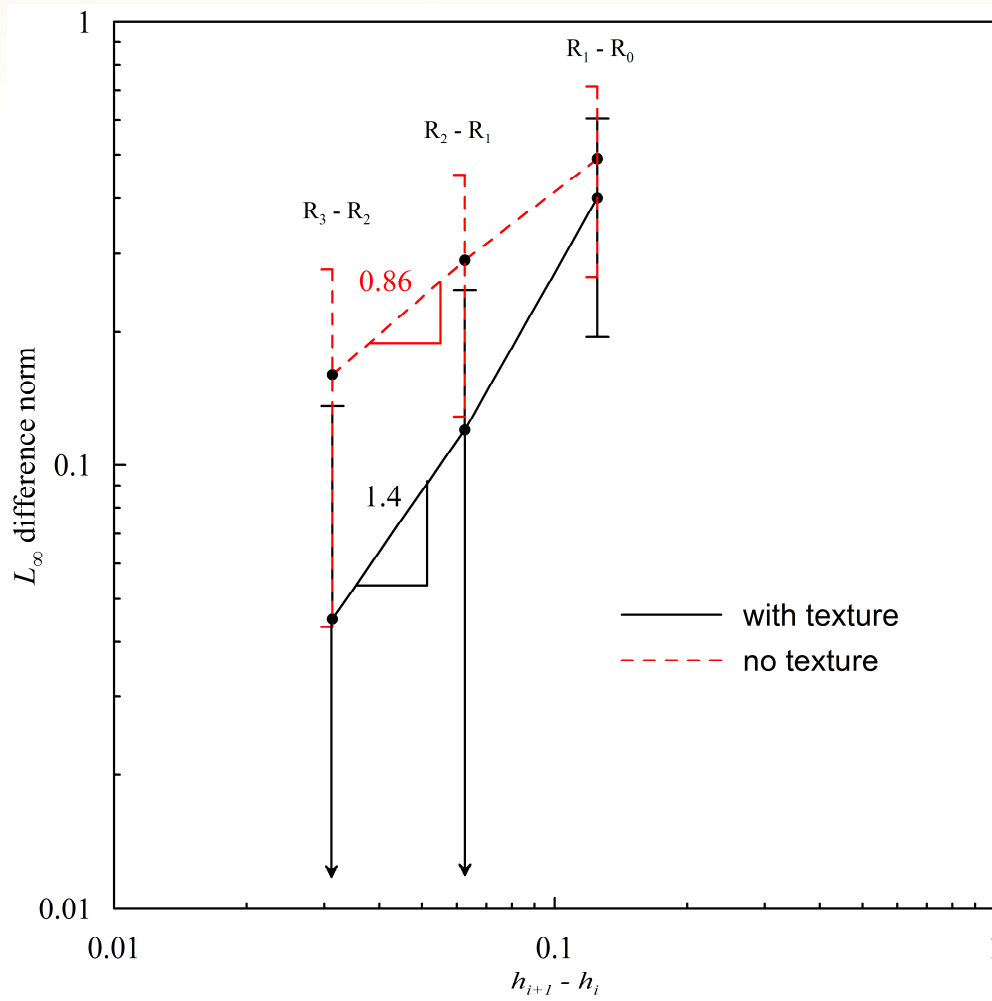
$$N_0 = 1714$$

$$N_1 = 2274$$

$$N_2 = 2386$$

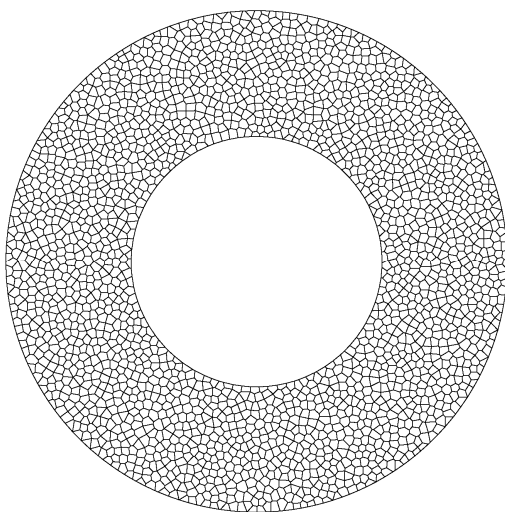
$$N_3 = 2421$$

Convergence in Distribution?

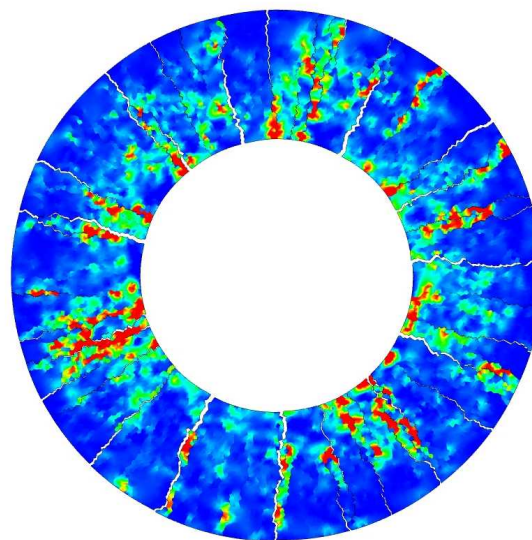


Example Revisited

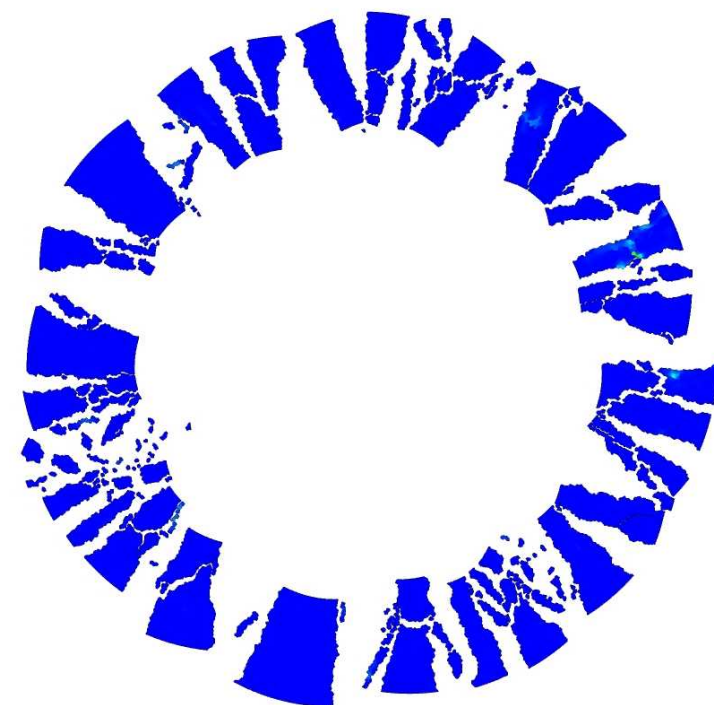
What about convergence?



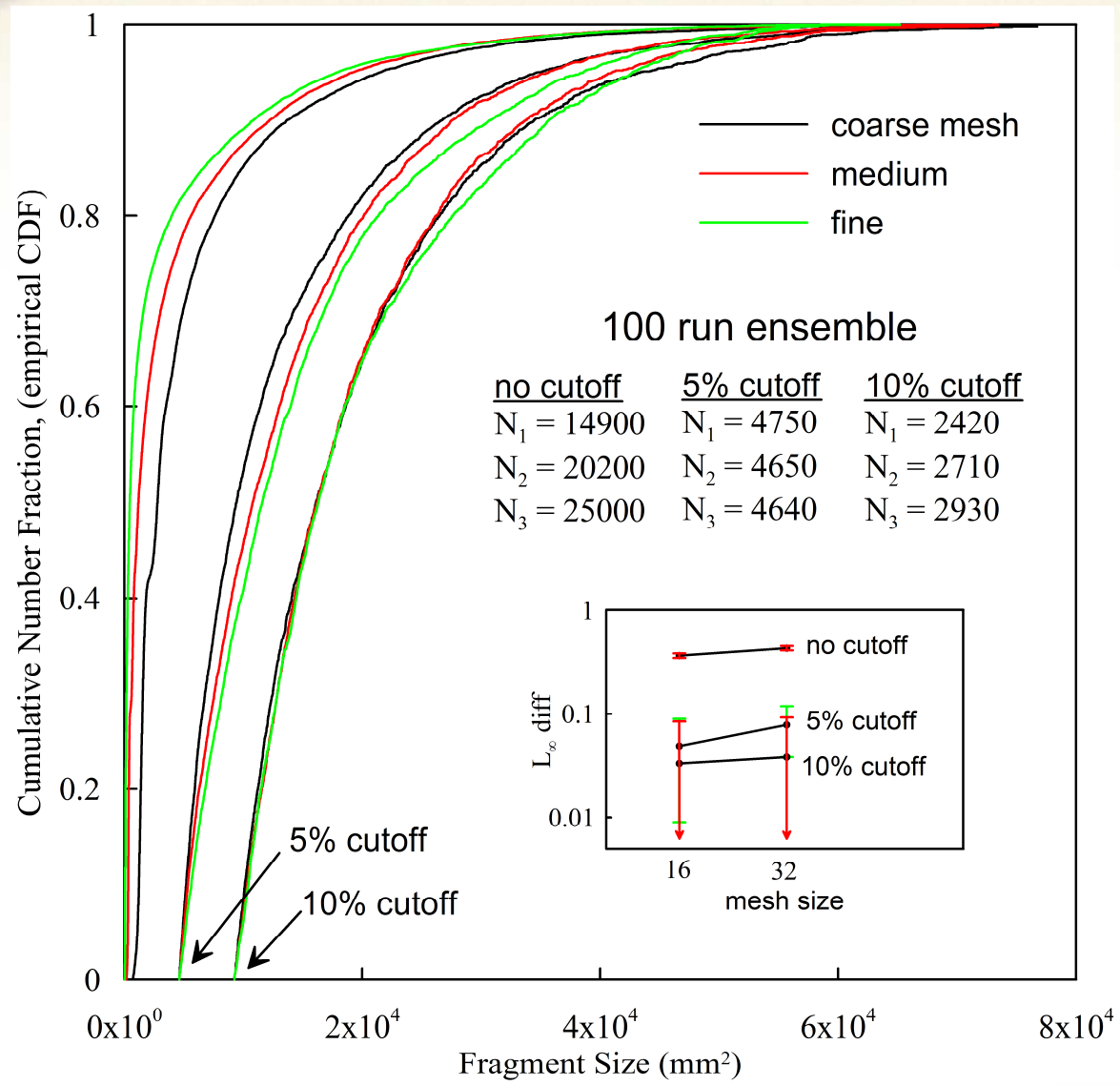
$t = 0$



$t = 2 \text{ ms}$

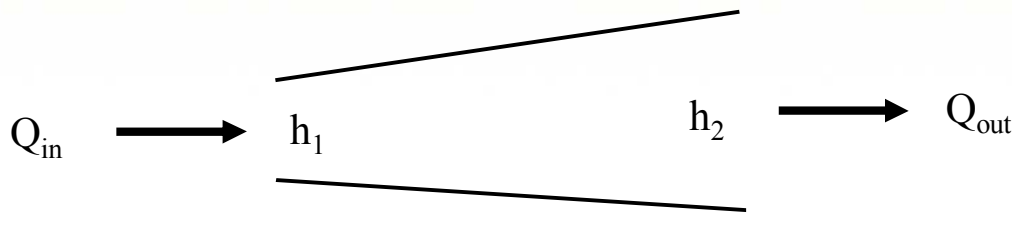


$t = 20 \text{ ms}$



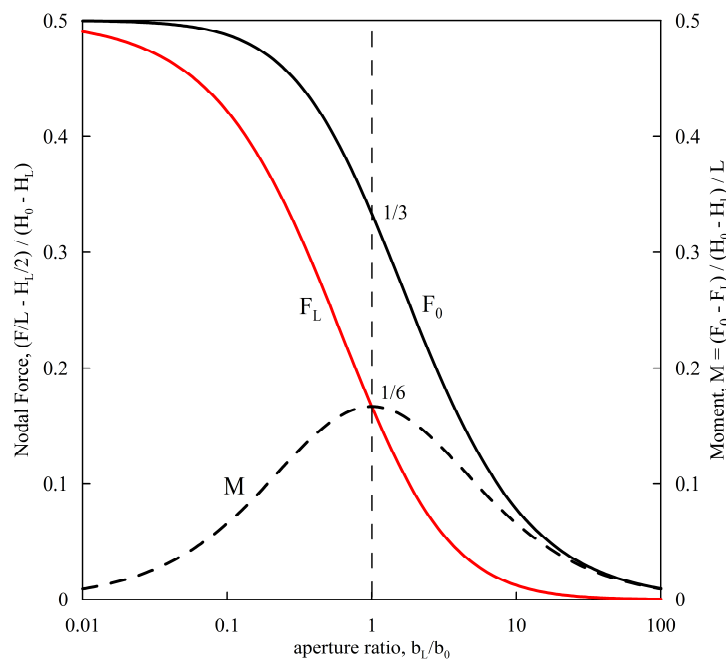
Application to Geo-Systems

fluid-flow in discrete fracture-networks

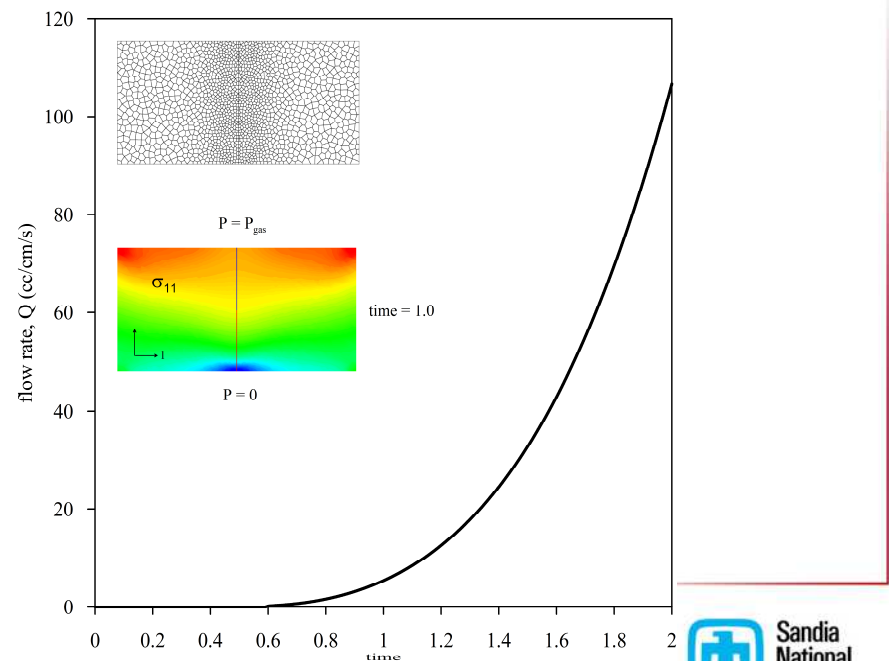


- Reynold's equation
- coupled fluid-structure
- solve fluid-network problem at each structural time step

Nodal Forces

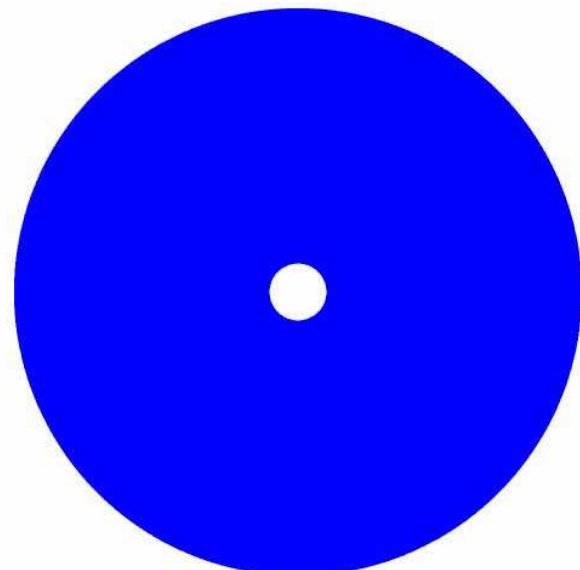


Flow Rate

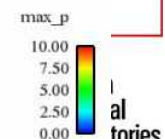
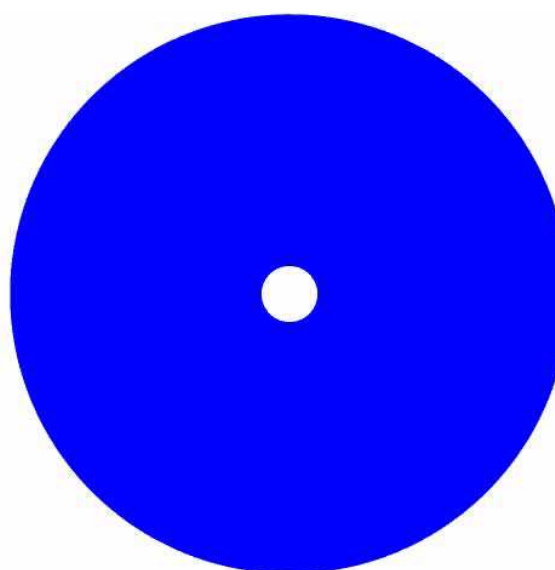
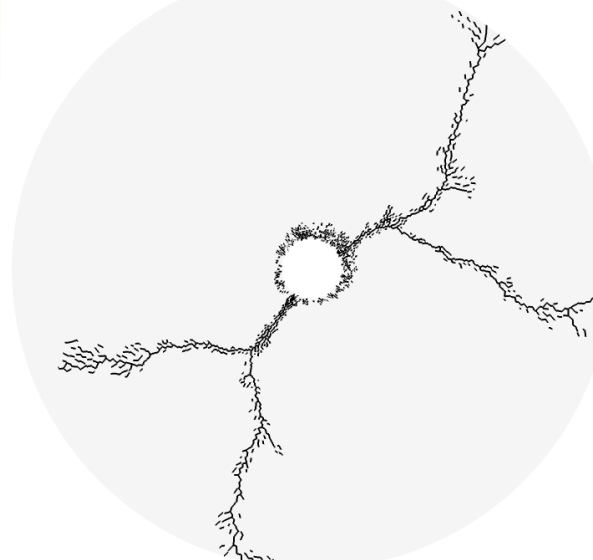


Hydrofrac Simulations

no fluid on crack faces



with fluid on crack faces





Summary

1. Development of arbitrary polyhedral finite elements.
2. Using randomly close-packed Voronoi meshes to model pervasive fracture in random media.
3. Statistical definitions of convergence.
4. Application to fragmentation and the modeling of fluid-structure coupling in geo-systems with discrete fracture networks.